Computational Fluid Flow Analysis of Cryogenic Turboexpander

A Thesis Submitted in Partial Fulfilment

of the Requirements for the Award of the Degree of

Master of Technology

in

Thermal Engineering

by

Hitesh Dimri

Department of Mechanical Engineering
National Institute of Technology, Rourkela
Rourkela-769008, Odisha, INDIA

May 2013

Computational Fluid Flow Analysis of Cryogenic Turboexpander

A Thesis Submitted in Partial Fulfilment

of the Requirements for the Award of the Degree of

Master of Technology

in

Thermal Engineering

by

Hitesh Dimri
(Roll – 211ME3188)

Under the Guidance of

Prof. Ranjit Kumar Sahoo

Department of Mechanical Engineering
National Institute of Technology, Rourkela
Rourkela-769008, Odisha, INDIA
2011-2013

DEPARTMENT OF MECHANICAL ENGINEERING
NATIONAL INSTITUTE OF TECHNOLOGY
ROURKELA, ODISHA-769008

CERTIFICATE

This is to certify that the thesis entitled "**Computational Fluid Flow Analysis of Cryogenic Turboexpander**" by **Hitesh Dimri**, submitted to the National Institute of Technology (NIT), Rourkela for the award of Master of Technology in **Thermal Engineering**, is a record of bona fide research work carried out by him in the Department of Mechanical Engineering, under my supervision and guidance.

I believe that this thesis fulfills part of the requirements for the award of degree of Master of Technology. The results embodied in the thesis have not been submitted for the award of any other degree elsewhere.

Place: Rourkela

Date:

Prof. Ranjit Kumar Sahoo
Department of Mechanical Engineering
National Institute of Technology
Rourkela Odisha-769008

ACKNOWLEDGEMENT

I am extremely fortunate to be involved in an exciting and challenging research project like "**Computational Fluid Flow Analysis of Cryogenic Turboexpander**". It has enriched my life, giving me an opportunity to work in a new environment of ANSYS CFX. This project increased my thinking and understanding capability as I started the project from scratch.

I would like to express my gratitude and respect to my supervisor **Prof. Ranjit Kumar Sahoo**, for his excellent guidance, valuable suggestions and endless support. He has not only been a wonderful supervisor but also a genuine person. I consider myself extremely lucky to be able to work under guidance of such a dynamic personality. Actually he is one of such genuine person for whom my words will not be enough to express.

I would like to express my sincere thanks to **Mr. Balaji** and **Mr. Sachindra** for their precious suggestions and encouragement to perform the project work. They were very patient to hear my problems that I am facing during the project work and finding the solutions. I am very much thankful to them for giving their valuable time for me.

I would like to express my thanks to all my classmates, all staffs and faculty members of mechanical engineering department for making my stay in N.I.T. Rourkela a pleasant and memorable experience and also giving me absolute working environment where I unlashed, my potential.

Date:

Hitesh Dimri
Roll. No. 211ME3184
M.Tech. (Thermal Engineering)

ABSTRACT

Cryogenic turboexpander is the most critical component of cryogenic plant to achieve low temperature refrigeration. A cryogenic turboexpander has many components like expansion turbine, compressor, heat exchanger, instrumentations etc. Expansion turbine is the component where temperature of gases decreases due to expansion and produce the coldest level of refrigeration in the plant.

This project deals with the computational fluid flow analysis of high speed expansion turbine. This involves with the three dimensional analysis of flow through a radial expansion turbine using nitrogen as flowing fluid. This analysis is done using cfd packages, bladegen, turbogrid and CFX. Bladegen is used to create the model of turbine using available data of hub, shroud and blade profile. Turbogrid is used to mesh the model. *CFX-Pre* is used to define and specify the simulation settings and physical parameters required to describe the flow through turboexpander at inlet and outlet. *CFX-Post* is used for examining and analyzing results. Using these results variation of different thermodynamic properties inside the turbine can be seen.

Various graphs are potted indicating the variation of velocity, pressure, temperature, entropy and Mach number along streamline and span wise to analyze the flow through cryogenic turbine.

Keywords: Radial turbine, Bladegen, Turbogrid, CFX.

CONTENTS

CERTIFICATE **i**

ACKNOWLEDGMENT **ii**

ABSTRACT **iii**

CONTENTS **iv**

LIST OF TABLES **vi**

LIST OF FIGURES **viii**

NOMENCLATURE **x**

CHAPTER 1: Introduction **1**

1.1 Overview of Turboexpander..... 2

1.2 Anatomy of a Cryogenic Turboexpander..... 3

1.3 Objective of the present investigation..... 4

1.4 Organization of the thesis 5

CHAPTER 2: Literature Review **6**

2.1 History of development 7

2.2 Design of turboexpander 11

CHAPTER 3: Theory **15**

3.1 Design of Turboexpander..... 16

3.1.1 Fluid parameters and layout of components 16

3.1.2 Design of turbine wheel 17

3.1.3 Determination of Blade Profile……... 18

CHAPTER 4: Computational Fluid Flow Analysis 21

4.1 Designing of Turboexpander in Bladegen ……. 22

4.2 Meshing of Model……... 25

4.3 Physics definition of Meshed Model in CFX-Pre..... 28

4.4 Obtaining a Solution Using CFX-Solver.……..…….. 30

4.5 Obtaining Results in CFX CFD-Post...……..…….. 32

CHAPTER 5: Results and Discussion 33

5.1 Pressure variation along streamwise inlet to outlet……...……. 35

5.2 Temperature variation along streamwise inlet to outlet……..... 36

5.3 Velocity variation along streamwise inlet to outlet…….…….……..... 38

5.4 Variation of Mach number along streamwise…….. 38

5.5 Variation of density along streamwise inlet to outlet…….. 39

5.6 Variation of Static Entropy along streamwise……. 40

5.7 Pressure variation along spanwise hub to shroud…… 41

5.8 Temperature variation along spanwise hub to shroud……. 42

5.9 Velocity variation along spanwise hub to shroud……... 43

5.10 Blade to blade plots for different spans……. 45

5.11 Meridional Plots…… 47

CHAPTER 6: Conclusions and Future Work 49

6.1 Conclusions...…….. 50

6.2 Future work…….…… 50

References 51

LIST OF TABLES

Table 3.1: Basic input parameters for the cryogenic expansion turbine system ……. 17

Table 3.2: Thermodynamic state at turbine outlet...……..... 18

Table 3.3: Thermodynamic state at turbine inlet …….. 18

Table 3.4: Coordinates for Generation of Blade Profile ……... 19

Table 3.5: Turbine blade profile co-ordinates of pressure and suction surfaces …..……. 20

Table 4.1: Physics definition for turbine rotor ……..…….. 29

Table 5.1: Variations of thermodynamic properties…….…….……. 34

LIST OF FIGURES

Figure 1.1: Division of cryogenic turboexpander …… 3

Figure 3.1: State points of turboexpander…….…….…… 17

Figure 4.1: Meridional blade profile with different spans……. 23

Figure 4.2: Variation of Beta and Theta at different spans along radius ……..……. 23

Figure 4.3: Variation of Beta and Theta …….……..... 24

Figure 4.4: Wireframe model of turbine generated in bladegen …… 24

Figure 4.5: Solid model of turbine generated in bladegen …….…… 25

Figure 4.6: Turbine rotor view after importing from Bladegen ……..…….. 26

Figure 4.7: Turbine rotor view after setting topology …… 27

Figure 4.8: Meshed 3D view of turbine rotor …….…….…….……. 28

Figure 4.9: Flow direction at inlet and outlet …… 30

Figure 4.10: Wireframe and Meridional model of turbine rotor …….……. 32

Figure 5.1: Pressure variation along streamwise inlet to outlet ……..…… 35

Figure 5.2: Isometric 3D view of pressure variation ……..……. 36

Figure 5.3: Temperature variation along streamwise inlet to outlet …….…... 37

Figure 5.4: Isometric 3D view of temperature variation ……..…… 37

Figure 5.5: Velocity variation along streamwise inlet to outlet …….……. 38

Figure 5.6: Variation of Mach number along streamwise …….…..……. 39

Figure 5.7: Variation of density along streamwise inlet to outlet …….……. 40

Figure 5.8: Variation of Static Entropy along streamwise ……...…….. 41

Figure 5.9: Pressure variation along spanwise hub to shroud ……..... 42

Figure 5.10: Temperature variation along spanwise hub to shroud ……..….. 43

Figure 5.11: Velocity variation along spanwise hub to shroud ……..……. 44

Figure 5.12: Velocity Vectors at 20% Span ……..…. 45

Figure 5.13: Velocity Vectors at 50% Span …… 45

Figure 5.14: Velocity Vectors at 80% Span ……... 46

Figure 5.15: Mass Averaged Pressure on Meridional Surface ……..….. 47

Figure 5.16: Mass Averaged Relative Mach number on Meridional Surface ……. 47

Figure 5.17: Velocity Streamlines at Blade Trailing Edge…….. 48

NOMENCLATURE

D	diameter (wheel)	(m)
d	diameter (shaft)	(m)
E	entropy	(J kg^{-1} K^{-1})
h	enthalpy	(J/kg)
K_e	free parameters	(dimensionless)
K_h	free parameters	(dimensionless)
M	mach number	(dimensionless)
N	rotational speed	(rev/min)
n_s	specific speed	(dimensionless)
P	pressure	(N/m^2)
Q	volumetric flow rate	(m^3/s)
r	radius	(m)
S_E	energy source	(kg m^{-1} s^{-3})
S_M	momentum source	(kg m^{-2} s^{-2})
T	temperature	(K)
t	blade thickness	(m)
U	velocity magnitude	(m/s)
Z	number of vanes	(dimensionless)

Greek symbols

ρ	density	(kg/m^3)
τ	shear stress	($kg\ m^{-1}\ s^{-2}$)
ω	rotational speed	(rad/s)
θ	tangential coordinate	(dimensionless)

Subscripts

0	stagnation condition
in	inlet to the nozzles
1	exit from the nozzles
2	inlet to the turbine wheel
3	exit from the turbine wheel

Chapter 1

INTRODUCTION

Chapter 1

1. INTRODUCTION:

1.1 Overview of Turboexpander:

Turboexpander are used in all areas of the gas and oil industries to produce cryogenic refrigeration. A turboexpander, on other hand, is a pressure let-down device that produces cryogenic temperature while simultaneously recovering energy from a plant stream in form of shaft power that can be used to drive other machinery such as compressor.

Though nature has provided an abundant supply of gaseous raw materials in the atmosphere (oxygen, nitrogen) and beneath the earth's crust (natural gas, helium), we need to harness and store them for meaningful use. In fact, the volume of consumption of these basic materials is considered to be an index of technological advancement of a society. For large-scale storage, transportation and for low temperature applications liquefaction of the gases is necessary. The only viable source of nitrogen, oxygen and argon is the atmosphere. For producing atmospheric gases like nitrogen, oxygen and argon in large scale, low temperature distillation provides the most economical route. The low temperature required for liquefaction of common gases can be obtained by several processes. While air separation plants, helium and hydrogen liquefiers based on the high pressure Linde and Heylandt cycles were common during the first half of the 20^{th} century, cryogenic process plants in recent years are almost exclusively based on the low-pressure cycles. They use an expansion turbine to generate refrigeration.

Compared to the high and medium pressure systems, turbine based plants have the advantage of high thermodynamic efficiency, high reliability and easier integration with other systems. The expansion turbine is the heart of a modern cryogenic refrigeration or separation system. Cryogenic process plants may also use reciprocating expanders in place of turbines. But with the improvement of reliability and efficiency of small turbines, the use of reciprocating expanders has largely been discontinued.

1.2 Anatomy of a Cryogenic Turboexpander:

The turboexpander essentially consists of a turbine wheel and a brake compressor mounted on a single shaft, supported by the required number of journal and thrust bearings. These basic components are held in place by an appropriate housing, which also contains the fluid inlet and exit ducts. The basic components are turbine wheel, brake compressor, shaft, nozzle, bearing, diffuser, seals, etc.

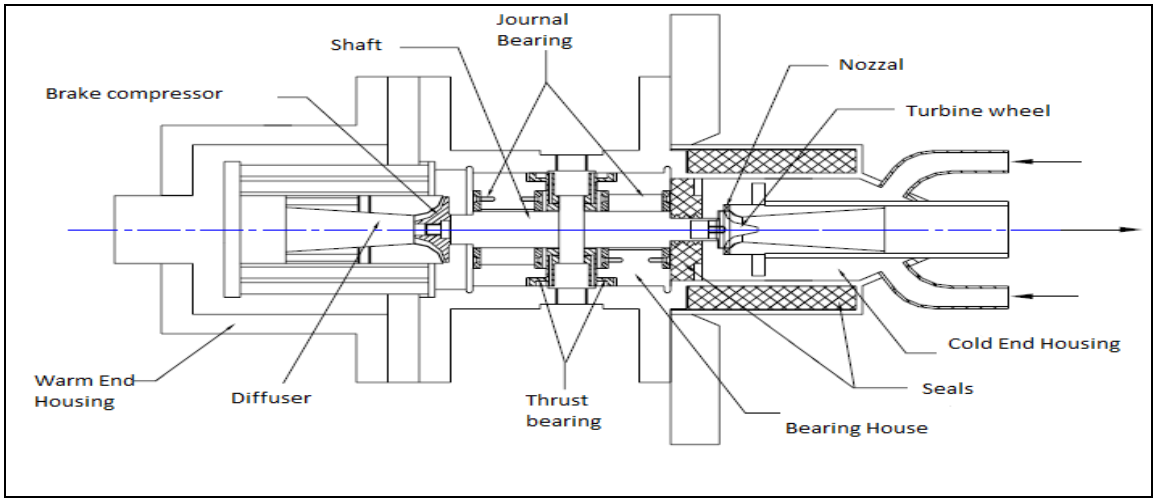

Figure1.1 Division of cryogenic turboexpander

Most of the rotors for small and medium sized plants are vertically oriented for easy installation and maintenance. It consists of a shaft with the turbine wheel fitted at one end and the brake compressor at the other. The high-pressure process gas enters the turbine through piping to the cold end housing and, from there, into the nozzle ring. The fluid accelerates through the converging passages of the nozzles. Pressure energy is transformed into kinetic energy, so that reduction in static temperature takes place. The high velocity gas streams impinge on the rotor blades, imparting force to the rotor and creating torque. The nozzles and the rotor blades are so aligned as to eliminate sudden changes in flow direction and consequent loss of energy. The turbine wheel is of radial or mixed flow geometry, i.e. the flow enters the wheel radially and exits axially. The blade passage has a profile of a three dimensional converging duct, changing from purely radial to an axial-tangential direction. Work is extracted as the process gas undergoes expansion with corresponding drop in static

temperature.

The diffuser is a diverging passage that converts most of the kinetic energy of the gas leaving the rotor to potential energy in the form of gain in pressure. Thus the pressure at the outlet of the rotor is lower than the discharge pressure of the turbine system. The expansion ratio in the rotor is thereby increased with a corresponding gain in cold production.

1.3 Objective of the present investigation:

Industrial gas manufactures in the technologically advanced countries have switched over from the high-pressure Linde and medium pressure reciprocating engine based Claude systems to the modern, expansion turbine based, low pressure cycles several decades ago. Thus in modern cryogenic plants a turboexpander is one of the most vital components- be it an air separation plant or a small reverse Brayton cryocooler.

For the development of computational fluid flow analysis of turboexpander system this project has been initiated. The objectives include: (i) building computational fluid dynamic knowledge base on cryogenic turboexpanders (ii) construction of a computational fluid flow model and study of its performance.

For the computational studies, a turboexpander system has been taken with the following specifications:

Working fluid : Nitrogen

Turbine inlet temperature : 99.65 K

Turbine inlet pressure : 3 bar

Turbine outlet pressure : 1.28 bar

Mass flow rate : 0.024kg/s

1.4 Organization of the thesis:

The thesis has been divided into six chapters. The first chapter presents a brief introduction to expansion turbines and their application in cryogenic process plants. Chapter–2 presents an extensive survey of available literature on various aspects of cryogenic turbine development.

The chapter-3 delivers a systematic design procedure based on published works that has been developed and documented for expansion turbine. In this chapter we discuss fluid parameters and layout of the components, design of turbine wheel and determination of blade profile from available research work.

Chapter-4 describes the computational set up to study the performance of the turbine. This chapter represents the designing of turbine in bladegen, meshing in turbogrid and simulation in CFX.

Simulated results for the expander have been included in this chapter-5. Various graphs and contours have been plotted in this chapter. Finally Chapter–6 is confined to some concluding remarks and for outlining the scope of future work.

*****

Chapter 2

LITERATURE REVIEW

Chapter 2

2. LITERATURE REVIEW

One of the main components of most cryogenic plants is the expansion turbine or the turboexpander. Since the turboexpander plays the role of the main cold generator, its properties– reliability and working efficiency, affect the cost effectiveness parameters of the entire cryogenic plant.

Due to their extensive practical applications, the turboexpander has attracted the attention of a large number of researchers over the years. Investigations involving experimental as well as theoretical studies have been reported in literature.

Journals such as Cryogenics and Turbomachinery and major conference proceedings such as Advances in Cryogenic Engineering and proceedings of the International Cryogenic Engineering Conference devote a sizable portion of their contents to research findings on turboexpander technology.

2.1 History of development

The concept that an expansion turbine might be used in a cycle for the liquefaction of gases was first introduced by Lord Rayleigh in a letter to "Nature" dated June 1898. He discussed the use of a turbine instead of a piston expander for the liquefaction of air. Rayleigh emphasized that the most important function of the turbine would be the refrigeration produced rather than the power recovered. In 1898, a British engineer named Edgar C. Thrupp patented a liquefying machine using an expansion turbine [1]. Thrupp's expander was a double-flow device with cold air entering the centre and dividing into two oppositely flowing streams. Joseph E. Johnson in USA patented an apparatus for liquefying gases. Joseph's expander was a De Laval or single stage impulse turbine. Other early patents include expansion turbines by Davis (1922). In 1934, a report was published on the first successful commercial application for cryogenic expansion turbine at the Linde works in Germany [2].

The single stage axial flow machine was used in a low pressure air liquefaction and separation cycle. It was replaced two years later by an inward radial flow impulse turbine.

The earliest published description of a low temperature turboexpander was by Kapitza in 1939, in which he describes a turbine attaining 83% efficiency. It had an 8 cm Monel wheel with straight blades and operated at 40,000 rpm [3]. In USA in 1942, under the sponsorship of the National Defence Research Committee a turboexpander was developed which operated without trouble for periods aggregating 2,500 hrs and attained an efficiency of more than 80% [3].

Work on the small gas bearing turboexpander commenced in the early fifties by Sixsmith at Reading University on a machine for a small air liquefaction plant [4]. In 1958, the United Kingdom Atomic Energy Authority developed a radial inward flow turbine for a nitrogen production plant [5]. During 1958 to 1961 Stratos Division of Fairchild Aircraft built blower loaded turboexpanders, mostly for air separation service [6]. Voth et. al developed a high speed turbine expander as a part of a cold moderator refrigerator for the Argonne National Laboratory (ANL) [7]. The first commercial turbine using helium was operated in 1964 in a refrigerator that produced 73 W at 3 K for the Rutherford helium bubble chamber [4].

A high speed turboalternator was developed by G. E. Co., New York in 1968, which ran on a practical gas bearing system capable of operating at cryogenic temperature with low loss [8-9]. National Bureau of Standards at Boulder, Colorado [10] developed a turbine with shaft diameter of 8 mm. This turbine operated at a speed of 600,000 rpm at 30 K inlet temperature. In 1974, Sulzer Brothers, Switzerland developed a turboexpander for cryogenic plants with self-acting gas bearings [11]. In 1981, Cryostar, Switzerland started a development program together with a magnetic bearing manufacturer to develop a cryogenic turboexpander incorporating active magnetic bearing in both radial and axial direction [12]. In 1984, the prototype turboexpander of medium size underwent extensive experimental testing in a nitrogen liquefier. Izumi et. al [13] at Japan developed a micro turboexpander for a small

helium refrigerator based on Claude cycle. This turboexpander consisted of a radial inward flow reaction turbine and a centrifugal brake fan on the lower and upper ends of a shaft supported by self-acting gas bearings. The turbine wheel diameter was 6mm and the shaft diameter was 4 mm. The rotational speeds of the 1^{st} and 2^{nd} stage turboexpander were 816,000 and 519,000 rpm respectively.

A simple method sufficient for the design of a high efficiency expansion turbine is outlined by Kun et. al [14-15]. Studies were initiated in 1979 to survey operating plants and generate the cost factors relating to turbine by Kun & Sentz [16]. Sixsmith et. al. [17] in collaboration with Goddard Space Centre of NASA, developed miniature turbines for Brayton Cycle cryocoolers. They have developed of a turbine with diameter 1.5 mm, rotating at a speed of approximately one million rpm [18].

Yang et. al [19] developed a two stage miniature expansion turbine made for 1.5 L/hr helium liquefier at the Cryogenic Engineering Laboratory of the Chinese Academy of Sciences. The turbines rotated at more and equal 500,000 rpm. The design of a small high speed turboexpander was taken up by the National Bureau of Standards (NBS) USA. The first expander operated at 600,000 rpm in externally pressurized gas bearings [20]. The turboexpander developed by Kate et. al [21] was with variable flow capacity mechanism (an adjustable turbine), which had the capacity of controlling the refrigerating power by using the variable nozzle vane height.

A wet type helium turboexpander with expected adiabatic efficiency of 70% was developed by the Naka Fusion Research Centre affiliated to the Japan Atomic Energy Institute [22-23]. The turboexpander consists of 59 mm impeller diameter, a 40 mm shaft, and self-acting gas journal and thrust bearings [22]. Ino et. al [24-25] developed a high expansion ratio radial inflow turbine for a helium liquefier of 100 L/hr capacity for use with a 70 MW superconductive generator. The turboexpander third stage was designed and manufactured in 1991, for the gas expansion machine regime, by “Cryogenmash” [26]. Each stage of the turboexpander design was similar, differing from one another by dimensions only produced

by “Heliummash” [26].

The ACD Company incorporated gas lubricated hydrodynamic foil bearings into a TC–3000 turboexpander [27]. Detailed specifications of the different modules of turboexpander developed by the company have been given in tabular format in Reference [28].

Agahi et. al. [29-30] have explained the design process of the turboexpander utilizing modern technology, such as CFD software, Computer Numerical Control Technology and Holographic Techniques to further improve an already impressive turboexpander efficiency performance. Improvements in analytical techniques, bearing technology and design features have made turboexpanders to be designed and operated at more favorable conditions such as higher rotational speeds. A Sulzer dry turboexpander, Creare wet turboexpander and IHI centrifugal cold compressor were installed and operated for about 8000 hrs in the Fermi National Accelerator Laboratory, USA [31]. This Accelerator Division/Cryogenics department is responsible for the maintenance and operation of both the Central Helium Liquefier (CHL) and the system of 24 satellite refrigerators which provide 4.5 K refrigeration to the magnets of the Tevatron Synchrotron. Theses expanders have achieved 70% efficiency and are well integrated with the existing system.

Sixsmith et. al. [32] at Creare Inc., USA developed a small wet turbine for a helium liquefier set up at the particle accelerator of Fermi National laboratory. The expander shaft was supported in pressurized gas bearings and had a turbine rotor of 4.76 mm at the cold end and a 12.7 mm brake compressor at the warm end. The turboexpander had a design speed of 384,000 rpm and a design cooling capacity of 444 Watts. Xiong et. al. [33] at the institute of cryogenic Engineering, China developed a cryogenic turboexpander with a 103 mm long rotor and weighing 0.9 N, which had a working speed up to 230,000 rpm. The turboexpander was experimented with two types of gas lubricated foil journal bearings. The L’Air company of France has been manufacturing cryogenic expansion turbines for 30 years and more than 350 turboexpanders are operating worldwide, installed on both industrial plants and research institutes [34-35]. These turbines are recognised by the use of hydrostatic gas

bearings, providing unique reliability with a measured Mean Time between failures of 45,000 hours.

India has been lagging behind the rest of the world in this field of research and development. Still, significant and decent progress has been made during the past two decades. In CMERI Durgapur, Jadeja et. al [36-37] developed an inward flow radial expansion turbine supported on gas bearings for cryogenic plants. This device gave stable rotation at about 40,000 rpm. This programme was, however, discontinued before any significant progress could be achieved. Another programme at IIT Kharagpur developed a turboexpander unit by using aerostatic thrust and journal bearings which had a working speed up to 80,000 rpm. The detailed summary of technical features of the cryogenic turboexpander developed in various laboratories has been given in the PhD dissertation of Ghosh [38]. Recently Cryogenic Technology Division, BARC developed Helium refrigerator capable of producing 1 kW at 20K temperature.

2.2 Design of turboexpander

The process of designing turbomachines is very seldom straightforward. The final design is usually the result of several engineering disciplines: fluid dynamics, stress analysis, mechanical vibration, tribology, controls, mechanical design and fabrication. The process design parameters which specify a selection are the flow rate, gas compositions, inlet pressure, inlet temperature and outlet pressure [39]. This section on design and development of turboexpander intends to explore the basic components of a turboexpander.

Turbine wheel

During the past two decades, performance chart has become commonly accepted mode of presenting characteristics of turbomachines [40]. Several characteristics values are used for defining significant performance criteria of turbomachines such as turbine velocity ratio, pressure ratio, flow coefficient factor and specific speed [40]. Balje has presented a simplified

method for computing the efficiency of radial turbomachines and for calculating their characteristics [41]. Similarity considerations offer a convenient and practical method to recognize major characteristics of turbomachinery. Similarity principles state that two parameters are adequate to determine major dimensions as well as the inlet and exit velocity triangles of the turbine wheel. The specific speed and the specific diameter completely define dynamic similarity.

Specific speed and specific diameter

The concept of specific speed was first introduced for classifying hydraulic machines. Balje [42] introduced this parameter in design of gas turbines and compressors. Values of specific speed and specific diameter may be selected for getting the highest possible polytropic efficiency and to complete the optimum geometry [39]. Specific speed is a useful single parameter description of the design point of a compressible flow rotodynamic machine [43]. A design chart that has been used for a wide variety of turbomachinery has been given by Balje [42, 44]. The diagram helps in computing the maximum obtainable efficiency and the optimum design geometry in terms of specific speed and specific diameter for constant Reynolds number and Laval number.

According to Rohlik [45], for radial flow geometry, maximum static and total efficiencies occur at specific speed values of 0.58 and 0.93. Luybli and Filippi [46] state that low specific speed wheels tend to have major losses in the nozzle and vaneless pace zones as well as in the area of the rotating disc where as high specific speed wheels tend to have more gas turning and exit velocity losses. The specific speed and specific diameter are often referred to as shape parameters. They are also sometimes referred to as design parameters, since the shape dictates the type of design to be selected. Corresponding approximately to the optimum efficiency [15] a cryogenic expander may be designed with selected specific speed is 0.5 and specific diameter is 3.75. Kun and Sentz [16] had taken specific speed of 0.54 and specific diameter of 3.72. Sixsmith and Swift [20] have designed a pair of miniature

expansion turbines for the two expansion stages with specific speeds 0.09 and 0.14 respectively for a helium refrigerator.

One major difficulty in applying specific speed criteria to gas turbines exists because of dependent on the Mach and Reynolds numbers that occur. For this reason the specific speed is not a parameter that satisfies the laws of dynamic similarity if the compressibility of the operating fluid cannot be ignored. Endeavors to relate the losses exclusively to specific speed, and using it as the sole criterion for evaluating a design are not only improper from a fundamental point of view but may also create a false opinion about the state of the art, thereby hindering or preventing research work that establishes sound design criteria. Vabra [47] has suggested improvement of these charts by incorporating new data obtained through experiments. He has shown that optimum turbine performance can be expected at values of specific speed between 0.6 and 0.7 and the operating range for radial turbines may lie between specific speed values of 0.4 to 1.2.

Parameters

The ratio of exit tip to rotor inlet diameter should be limited to a maximum value of 0.7 to avoid excessive shroud curvature. Similarly, the exit hub to the tip diameter ratio should have a minimum value of 0.4 to avoid excessive hub blade blockage and loss [43, 45]. Kun and Sentz [16] have taken $\varepsilon = 0.68$. Balje [41] has taken the ratio of exit meridian diameter to inlet diameter of a radial impeller as 0.625. The inlet blade height to inlet blade diameter of the turbine wheel would lie between values of 0.02 to 0.6 [43]. The detailed design parameters for a 90° inward radial flow turbine is shown in Table 2.2 of the PhD dissertation of Ghosh [38].

The peripheral component of absolute velocity at the inlet of turbine wheel is mainly dependent upon the nozzle angle. The peripheral component of absolute velocity at the exit of turbine wheel is a function of the exit blade angle and the peripheral speed at the outlet [41]. Balje [41] shows that the desirable ratio of meridional component of absolute velocity at

the inlet and exit of the turbine wheel is a function of the flow factor and Mach number. He has taken the value of the ratio of Meridional components of absolute velocity at exit and inlet for a radial turbine as 1.0. Whitfield [48] has shown that for any given incidence angle, the absolute flow angle can be selected to minimize the absolute Mach number. The general view is that the optimum incidence angle is a function of the number of blades and lies between -20° and -30°.

Number of blades

Assuming a simplified blade loading distribution, Balje has derived an equation for the minimum rotor blade number as a function of specific speed. Denton [49] has given guidance on the choice of number of blades. By using his theory it can be ensured that the flow does not stagnate on the pressure surface. He suggests that a number of 12 blades is typical for cryogenic turbine wheels. Wallace [50] has given some useful information on best number of blades to avoid excessive frictional loss on the one hand and excessive variation of flow conditions between adjacent blades on the other.

Rohlik [45] recommends a procedure to estimate the required number of blades considering the criterion of flow separation in the rotor passage. In his formula, the number of blades is chosen so as to inhibit boundary layer growth in the flow passage. Sixsmith [10] used twelve complete blades and twelve partial blades in his turbine designed for medium size helium liquefiers. The blade number is calculated from the value of slip factor [36]. The number of blades must be so adjusted that the blade width and thickness can be manufactured with the available machine tools.

*****

Chapter 3

THEORY

3. THEORY

3.1 Design of Turboexpander

In this chapter the process of designing the experimental turboexpander and associated units for cryogenic process have been analyzed. The design procedure of the cryogenic turboexpander depends on working fluid, flow rate, inlet conditions and expansion ratio. The procedure created in this chapter allows any arbitrary combination of fluid species, inlet conditions and expansion ratio, since the fluid properties are adequately taken care in the relevant equations. The computational process is illustrated with examples. The present design procedure is available in literature [55]. The design methodology of the turboexpander system consists of the following units, which are described in the subsequent sections.

- Fluid parameters and layout of the components
- Design of turbine wheel
- Determination of blade profile

3.1.1 Fluid parameters and layout of components

The fluid specifications have been dictated by the requirements of a small refrigerator producing less than 1 KW of refrigeration. The inlet temperature has been specified rather arbitrarily, chosen in such a way that even with ideal (isentropic) expansion; the exit state should not fall in the two-phase region. The basic input parameters for the system are given in Table 3.1.

Table 3.1: Basic input parameters for the cryogenic expansion turbine system

Working fluid : Nitrogen	Discharge pressure : 1.27 bar
Turbine inlet temperature: 99.65K	Mass flow rate : 0.025 kg/s
Turbine inlet pressure : 3bar	

3.1.2 Design of turbine wheel

The design of turbine wheel has been done following the method outlined by Balje [8] and Kun & Sentz [29], which are based on the well-known " similarity principles". The similarity laws state that for given Reynolds number, Mach number and Specific heat ratio of the working fluid, to achieve optimized geometry for maximum efficiency, two dimensionless parameters: specific speed and specific diameter uniquely determine the major dimensions of the wheel and its inlet and exit velocity triangles. Specific speed (n_S) and specific diameter (d_S) are defined as:

Specific speed
$$n_s = \frac{\omega \times \sqrt{Q_3}}{(\Delta h_{in-3s})^{3/4}} \tag{3.1}$$

Specific diameter
$$d_s = \frac{D_2 \times (\Delta h_{in-3s})^{1/4}}{\sqrt{Q_3}} \tag{3.2}$$

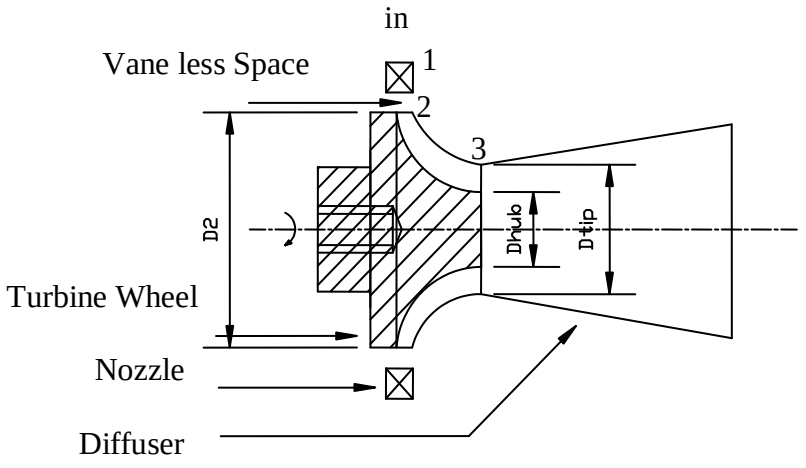

State points	
In	Nozzle inlet
1	Nozzle outlet
2	Turbine inlet
3	Turbine outlet

Figure3.1 State points of turboexpander

In summary, the major dimensions for prototype turbine have been computed by S.K. Ghosh [52] as follows:

Rotational speed: N = 22910rad/sec = 218790rpm

Wheel diameter: D_2 = 16.0 mm

Eye tip diameter: D_{tip} = 10.8mm

Eye hub diameter: D_{hub} = 4.6mm

Numbers of blades: Z_{tr} = 10

Thickness of blades: t_{tr} = 0.6mm

Thermodynamic state at wheel discharge (state 3):-

Thermodynamic state at turbine wheel outlet calculated by S. K. Ghosh [52] is in table3.2.

Table 3.2 Thermodynamic state at turbine outlet

	Stagnation value	Static value
Pressure (bar)	1.505	1.29
Entropy (kJ/kg.K)	5.452	5.452
Temperature (K)	90.02	85.96
Density (kg/m^3)	5.89	5.26

Thermodynamic state at wheel inlet (state 2)

Table 3.3 Thermodynamic state at turbine inlet

	Stagnation value	Static value
Pressure (bar)	2.872	2.453
Entropy (kJ/kg.K)	5.335	5.335
Temperature (K)	99.65	90.45
Density (kg/m^3)	10.312	9.728

3.1.3 Determination of Blade Profile:

The detailed procedure describes computation of the three dimensional contours of the blades and simultaneously determines the velocity, pressure and temperature profiles in the turbine wheel. The computational procedure suggested by Hasselgruber [51] and extended by Kun &

Sentz [16] has been adopted. The fluid pressure loss in a turbine blade passage depends on the length and curvature of the flow path. Thus two parameters K_e and K_h defined by Hasselgruber [51] control the flow path and its curvature. The magnitude of the velocity and change in its direction determine the optimum blade profile of the turbine. For the turbine blade design K_e varies between 0.75 and K_h 1 varies between 1 and 20.

Analysis of results done by S. K. Ghosh [53] reveal that an optimum combination of parameters K_e= 0.75 and K_h= 5.0 leads to a batter blade profile for turboexpander. The blade profile co-ordinate of mean surface, pressure surface and suction surface are shown in the Table 4.3 and Table 4.4 respectively.

Table 3.4 Coordinates for Generation of Blade Profile

Tip Camber line			Hub Camber line		
z(mm)	r(mm)	θ (deg)	z(mm)	r(mm)	θ (deg)
-0.24	5.38	0	0.24	2.32	0
0.24	5.29	6.71	0.67	2.56	6.71
0.71	5.22	12.39	1.11	2.76	12.39
1.18	5.19	17.19	1.55	2.94	17.19
1.63	5.18	21.22	2	3.1	21.22
2.08	5.19	24.58	2.46	3.25	24.58
2.52	5.22	27.37	2.93	3.4	27.37
2.95	5.27	29.65	3.39	3.56	29.65
3.37	5.33	31.49	3.86	3.72	31.49
3.79	5.41	32.96	4.33	3.91	32.96
4.19	5.51	34.1	4.79	4.13	34.1
4.58	5.63	34.96	5.24	4.37	34.96
4.97	5.78	35.61	5.68	4.65	35.61
5.34	5.95	36.06	6.09	4.97	36.06
5.69	6.16	36.38	6.47	5.32	36.38
6.02	6.4	36.58	6.81	5.7	36.58
6.33	6.68	36.7	7.11	6.11	36.7
6.62	6.99	36.77	7.37	6.54	36.77
6.87	7.33	36.8	7.59	6.99	36.8
7.09	7.7	36.81	7.76	7.45	36.81
7.28	8.1	36.81	7.9	7.92	36.81

Table 3.5 Turbine blade profile co-ordinates of pressure and suction surfaces

$z_{pressure}$(mm)	$r_{pressure}$(mm)	$\theta_{pressure}$(rad)	$z_{suction}$ (mm)	$r_{suction}$(mm)	$\theta_{suction}$(rad)
0	3.85	0.055	0	3.85	-0.055
0.45	3.92	0.166	0.45	3.92	0.068
0.91	3.99	0.26	0.91	3.99	0.172
1.36	4.07	0.339	1.36	4.07	0.261
1.82	4.14	0.404	1.82	4.14	0.336
2.27	4.22	0.458	2.27	4.22	0.4
2.72	4.31	0.502	2.72	4.31	0.453
3.17	4.41	0.537	3.17	4.41	0.497
3.62	4.53	0.566	3.62	4.53	0.533
4.06	4.66	0.588	4.06	4.66	0.562
4.49	4.82	0.605	4.49	4.82	0.585
4.91	5	0.617	4.91	5	0.603
5.32	5.21	0.627	5.32	5.21	0.616
5.71	5.46	0.633	5.71	5.46	0.626
6.08	5.74	0.637	6.08	5.74	0.633
6.42	6.05	0.64	6.42	6.05	0.637
6.72	6.39	0.641	6.72	6.39	0.64
6.99	6.77	0.642	6.99	6.77	0.641
7.23	7.16	0.642	7.23	7.16	0.642
7.43	7.58	0.642	7.43	7.58	0.642
7.59	8.01	0.642	7.59	8.01	0.642

******

Chapter 4

COMPUTATIONAL FLUID FLOW ANALYSIS

4. COMPUTATIONAL FLUID FLOW ANALYSIS

Computational fluid flow analysis of turboexpander can be done in three steps. Bladegen is used to create the model of turbine using available data of hub, shroud and blade profile. Turbogrid is used to mesh the model. CFX-Pre is used to define and specify the simulation settings and physical parameters required to describe the flow through turboexpander at inlet and outlet. CFX-Post is used for examining and analyzing results.

4.1. Designing of Turboexpander in Bladegen

ANSYS BladeGen is a geometry creation tool that is specialized for turbomachinery blades. Bladegen designing of model is done by using available hub, shroud and blade profile coordinates. The hub and the tip streamlines are available in the previous chapter. A surface is created by joining the hub and tip streamlines with a set of tie lines. BladeEditor will loft the blade surfaces in the streamwise direction through curves that run from hub to shroud. The surface so generated is considered as the mean surface within a blade. Non Uniform Rational B Splines are used to develop the solid surface. The suction and pressure surfaces of two adjacent channels are computed by translating the mean surface in the positive and negative theta direction through half the blade thickness.

After making all the surfaces when blade merge topology property is used, then blade faces will be merged where they are tangent to one another. Create fluid zone property is selected, to create a stage fluid zone body for the flow passage, and an enclosure feature to subtract the blade body. This resulting enclosure can be used for a CFD analysis of the blade passage. Create all blades this property is used to create all the blades using the number of blades specified in the Bladegen model. Here we are using ten numbers of blades.

Different views and curves of radial expansion turbine in bladegen are as following.

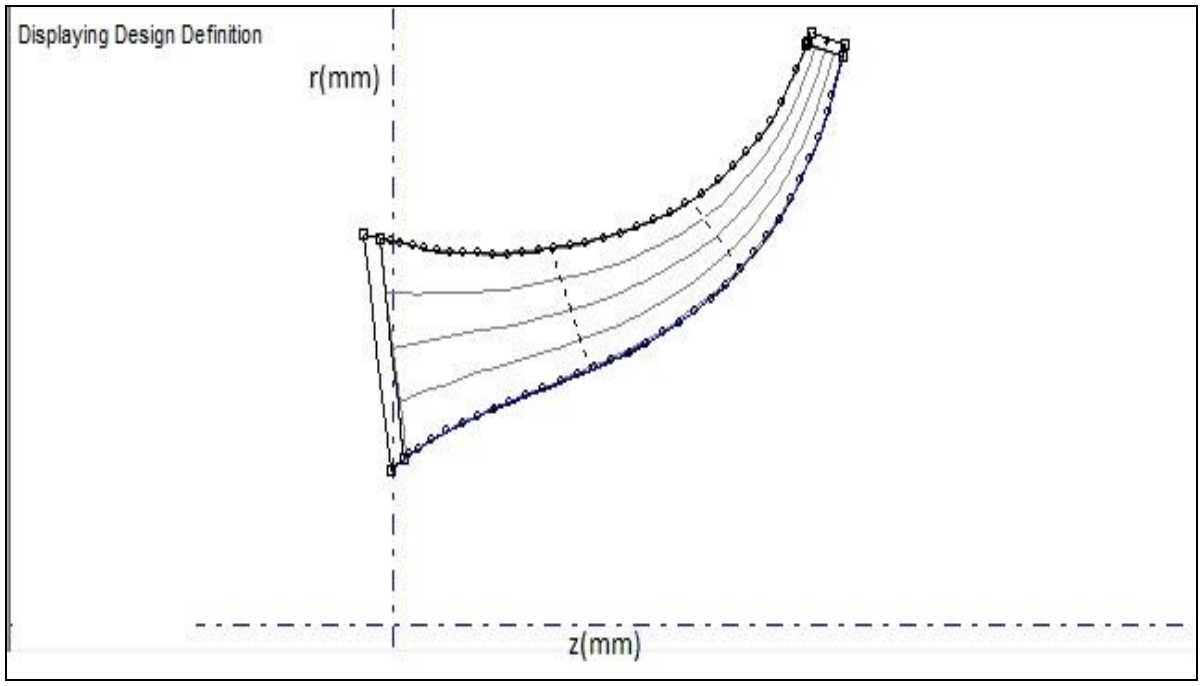

Figure 4.1: Meridional blade profile with different spans

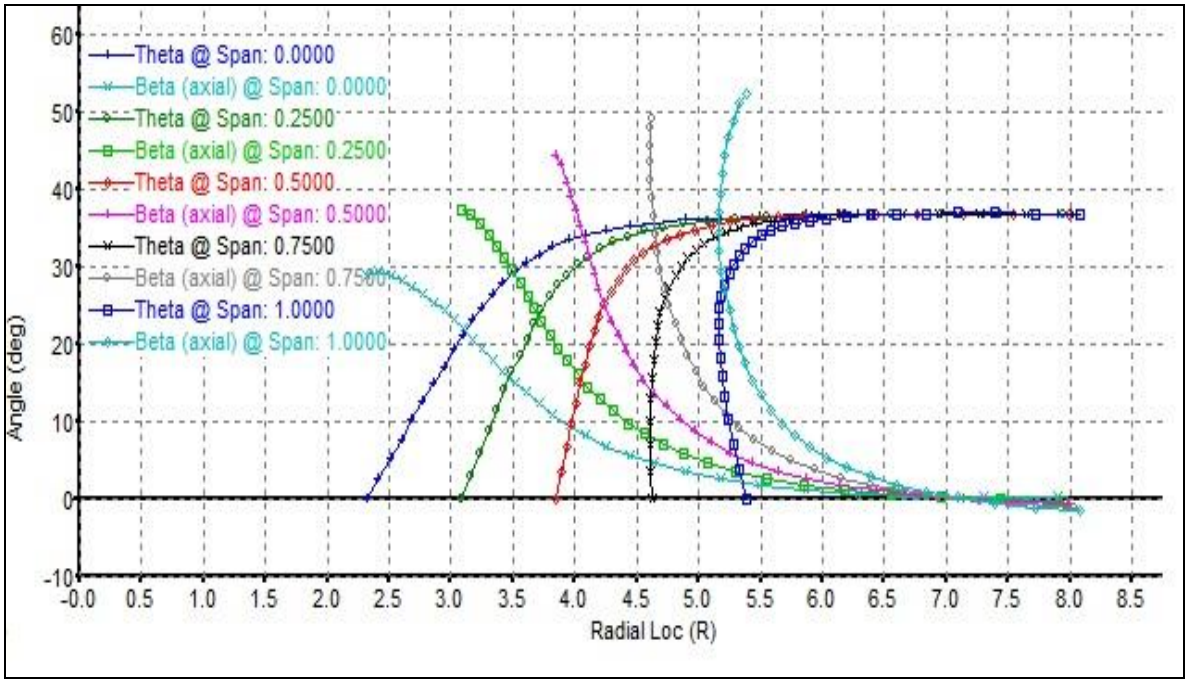

Figure 4.2: Variation of Beta and Theta at different spans along radius

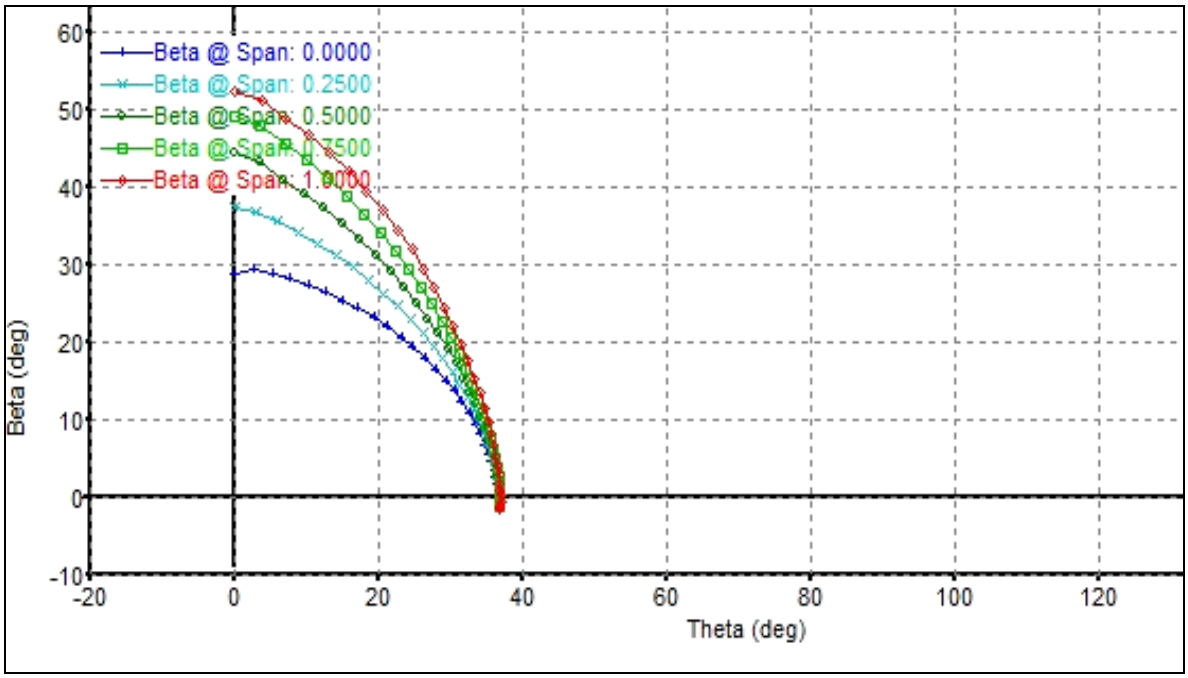

Figure 4.3: Variation of Beta and Theta

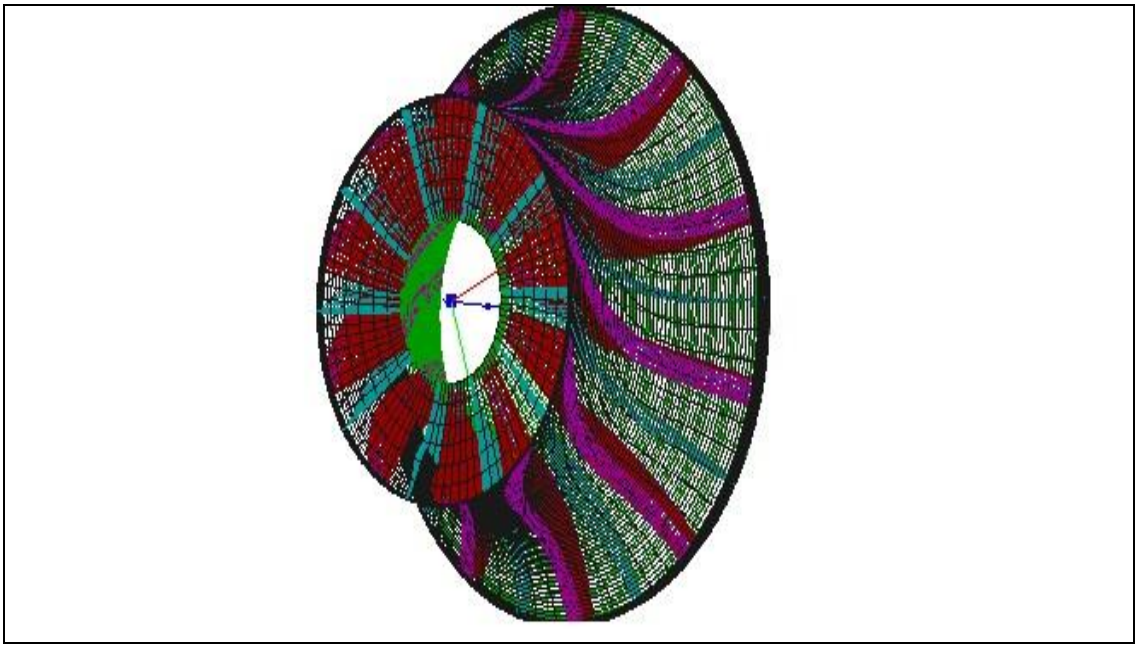

Figure 4.4: Wireframe model of turbine generated in bladegen

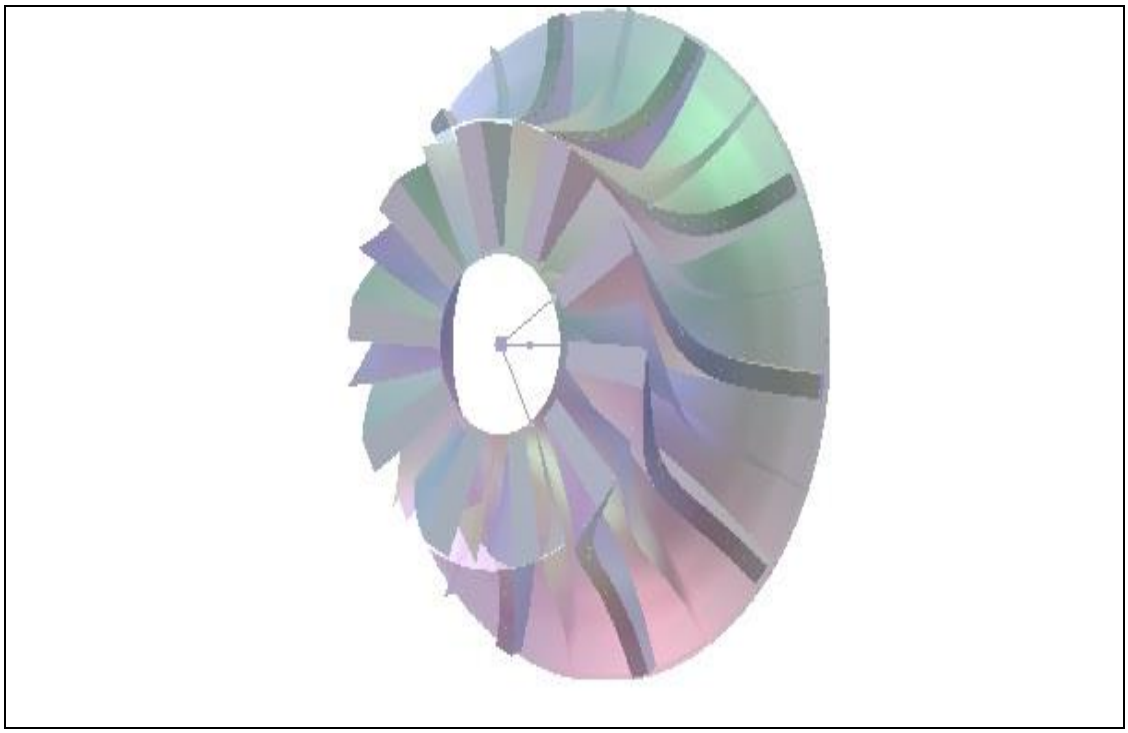

Figure 4.5: Solid model of turbine generated in bladegen

4.2. Meshing of Model:

Meshing of model is done in turbogrid. It creates high quality hexahedral meshes that are tuned to the demands of fluid dynamic analysis in turbine rotor. Turbine rotor geometry information is imported from bladegen. Turbogrid uses this bladegen file to set the axis of rotation, the number of blades, and a length unit that characterizes the scale of the machine. Machine data gives the basic information about the geometry. Here units specified for base units represent the scale of the geometry being meshed, these units are not used for importing geometric data nor do they govern the units written to a mesh file, they are used for the internal representation of the geometry to minimize computer round-off errors. To complete the geometry a small gap of 1 mm is created between the blade and the shroud.

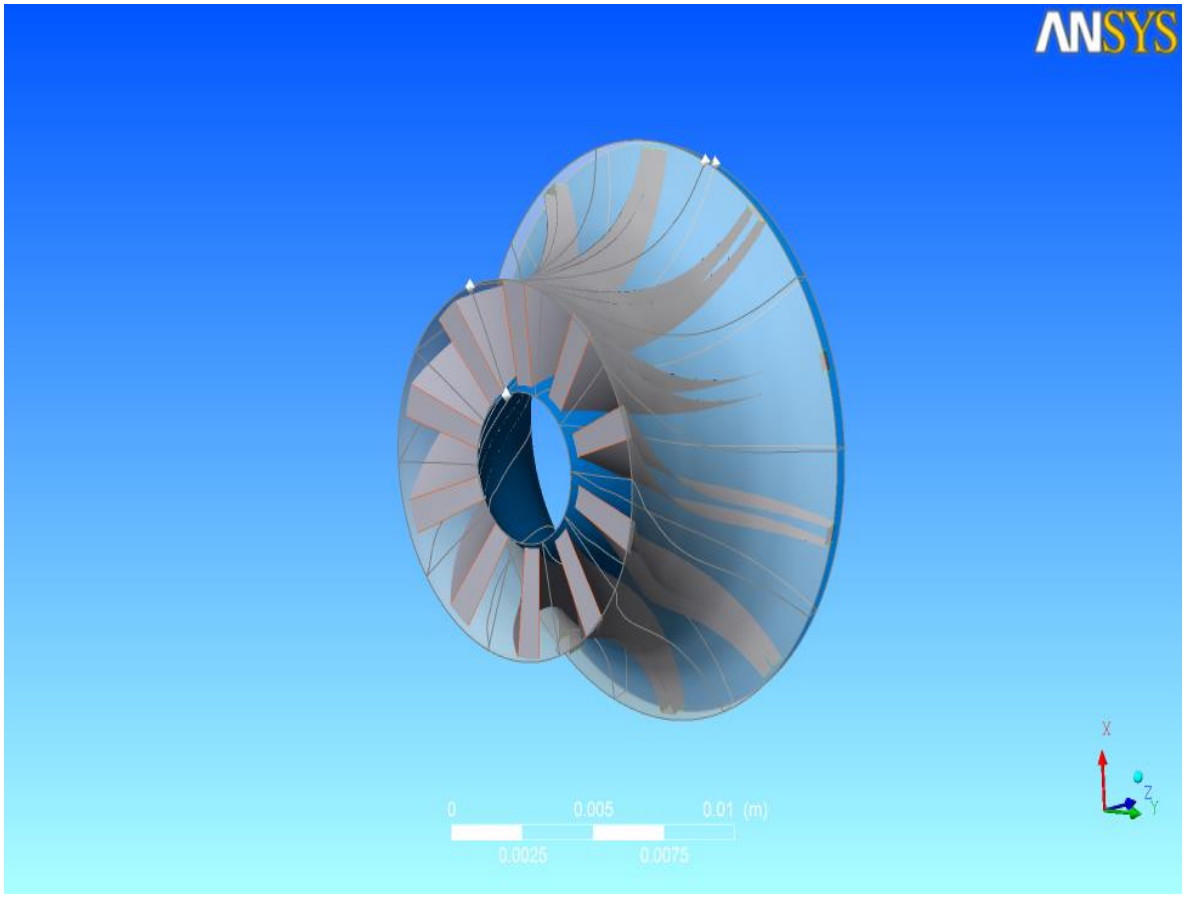

Figure 4.6: Turbine rotor view after importing from Bladegen

Next step is to create the topology that guides the mesh. Topology definition, placement to traditional with control points provides access to the legacy topology methods. Here H/J/C/L-Grid method is used to create mesh. The H/J/C/L-Grid method causes ANSYS Turbogrid to choose an H-Grid, J-Grid, C-Grid, L-Grid, or a combination of these, based on heuristics. In this case, the H/J/C/L-Grid method causes ANSYS Turbogrid to choose an H-Grid topology for the upstream end of the passage, and an H-Grid topology for the downstream end. Include O-Grid with 0.5 width factor is selected to add an O-Grid (thickness equal to half the average blade thickness) around the blade to increase mesh orthogonality in that region.

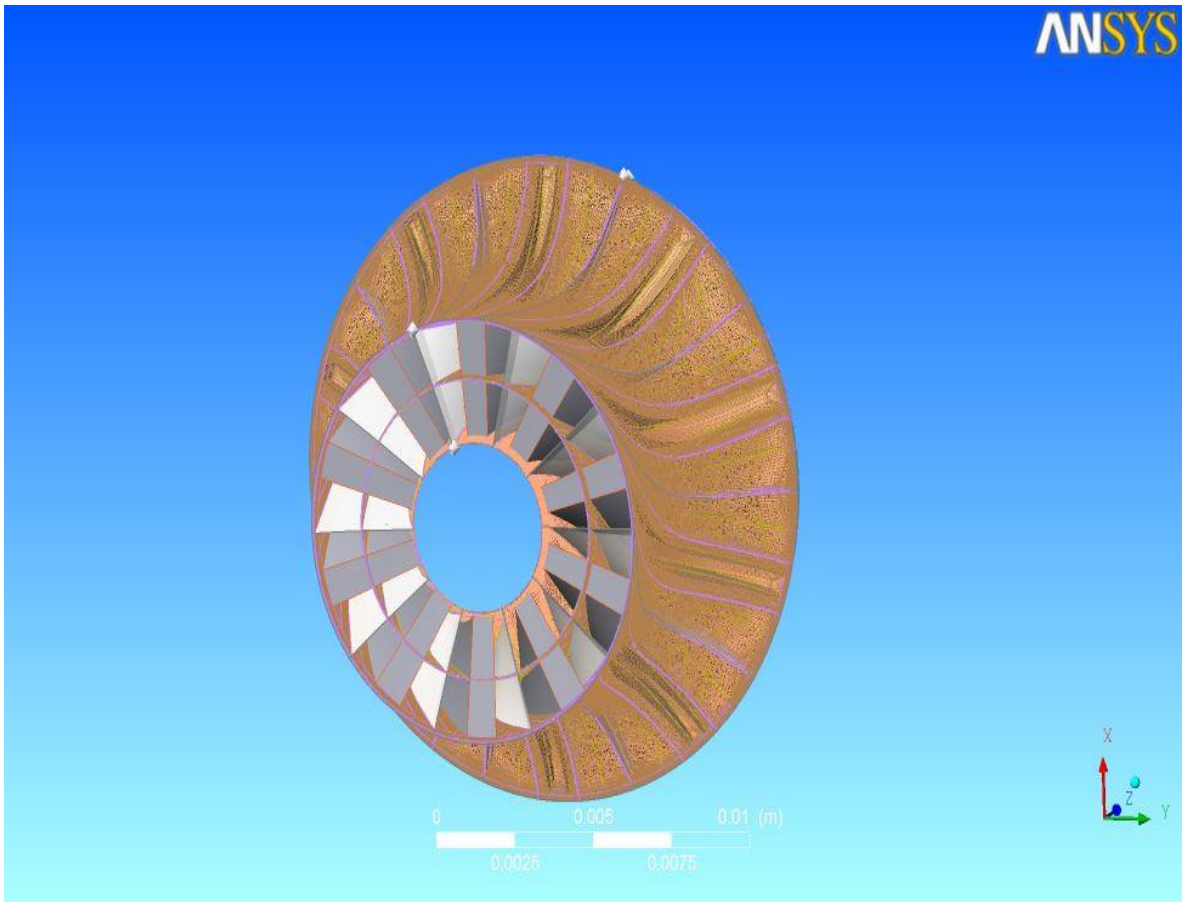

Figure 4.7: Turbine rotor view after setting topology

After setting topology definition, mesh data setting is used to control the number and distribution of mesh elements. Here we set the target number of nodes to 250000 to produce a fine mesh. Before generating the 3D mesh, mash quality should check on the layers, especially the hub and shroud tip layers. After correcting mash quality on layers, we generate the mesh with 228640 nodes and 206368 elements.

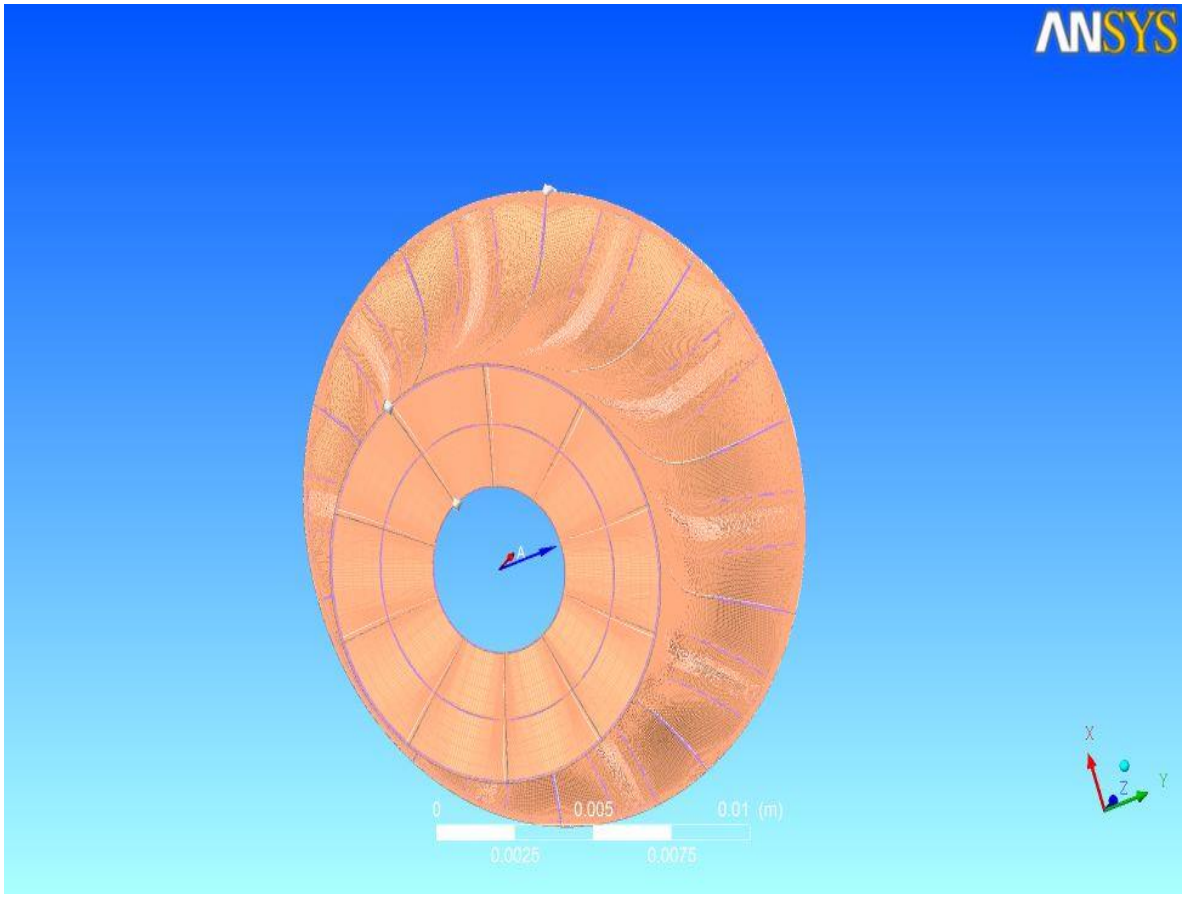

Figure 4.8: Meshed 3D view of turbine rotor

4.3. Physics definition of Meshed Model in CFX-Pre:

CFX-Pre is known as physics-definition pre-processor for ANSYS CFX. In cfx, turbo mode is used to define physic of meshed turbine rotor. Under basic setting in turbo mode, we set the machine type as radial turbine and rotation axis to z. In component definition we set component type rotating and set rotation value 218780 rev/min. Turbo mode will automatically select a list of regions that correspond to certain boundary types. This information should be reviewed in the Region Information section to ensure that all is correct. This information is used to set up boundary conditions and interfaces. In wall configuration option we set tip clearance at shroud.

Physics definition tab is used to set fluid type, analysis type, model data, inflow and outflow boundary templates and solver parameters. Physics definition used for turbine rotor is given in the table below.

Table 4.1: Physics definition for turbine rotor

Tab	**Setting**		**Values**
Physics Definition	Fluid		Nitrogen
	Analysis Type		Steady state
	Modal Data	Reference pressure	0 (Pa)
		Heat Transfer	Total Energy
		Turbulence	k-Epsilon
	Inflow/Outflow Boundary Templates		Mass Flow Inlet P-Static Outlet
	Inflow	T-Total	99.65k
		Mass Flow	Per Component
		Mass Flow Rate	0.002326 kg/sec
		Flow Direction	Normal to Boundary
	Outflow	P-Static	1.29 bar
	Solver Parameters	Advection Scheme	High Resolution
		Convergence control	Physical Timescale
		Physical Timescale	0.000004 s

After setting physics definition Cfx-Pre will try to create appropriate interfaces and boundary conditions using the region names presented previously in the region information.

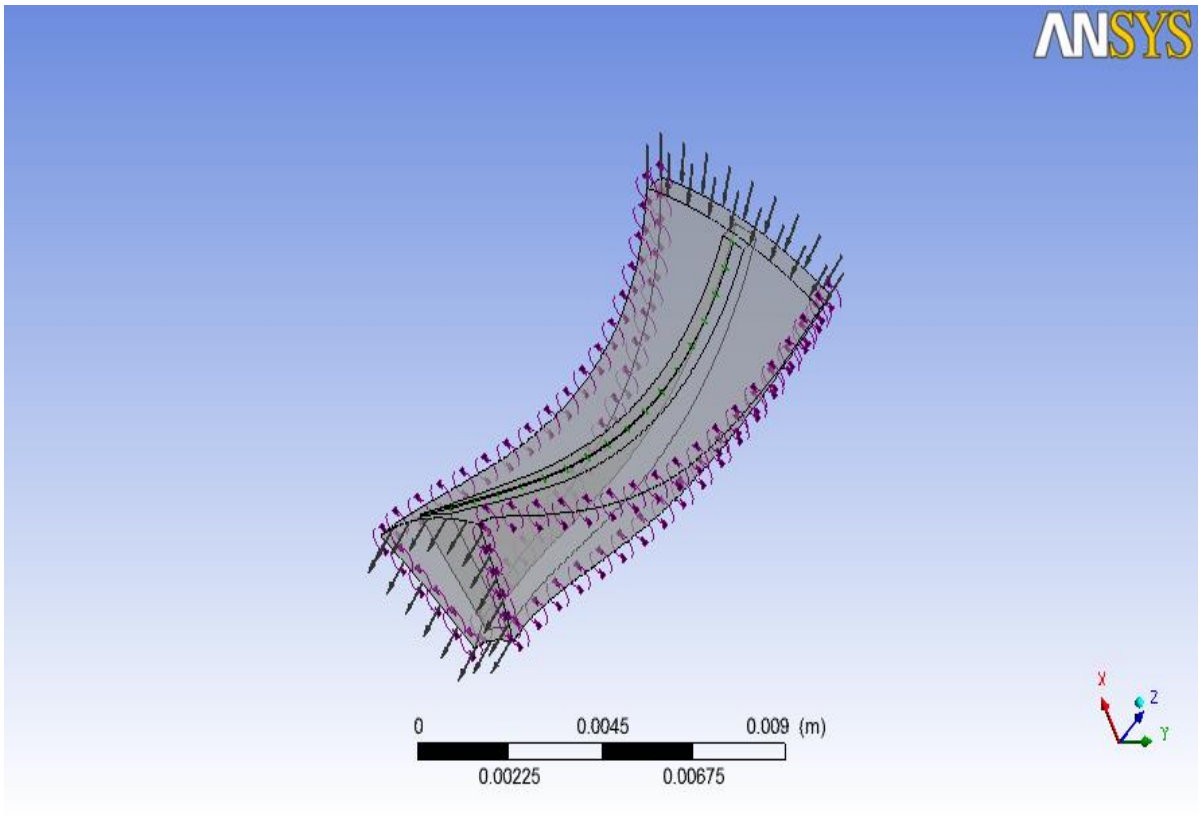

Figure 4.9: Flow direction at inlet and outlet

4.4. Obtaining a Solution Using CFX-Solver:

This chapter describes the mathematical equations used to model fluid flow, heat, and mass transfer in ANSYS CFX for single-phase, single and multi-component flow without combustion or radiation.

ANSYS CFX solves for the relative static pressure in the flow field, and is related to Absolute pressure.

$$P_{abs} = P_{ref} + P_{stat} \tag{4.1}$$

Specific static enthalpy is a measure of the energy contained in a fluid per unit mass. Static enthalpy is defined in terms of the internal energy of a fluid and the fluid state:

$$h_{stat} = u_{stat} + \frac{P_{stat}}{\rho_{stat}} \tag{4.2}$$

When we use the thermal energy model, the ANSYS CFX-Solver directly computes the static enthalpy.

The set of equations solved by ANSYS CFX are the unsteady Navier-Stokes equations in their conservation form. The instantaneous equations of mass, momentum and energy conservation can be written as follows in a stationary frame:

Continuity equation $$\frac{\partial \rho}{\partial t} + \nabla \bullet (\rho U) = 0 \quad (4.3)$$

Momentum equations $$\frac{\partial (\rho U)}{\partial t} + U \bullet (\rho U \otimes U) = -\nabla_p + \nabla \bullet \tau + S_M \quad (4.4)$$

Where the stress tensor, τ , is related to the strain rate by

$$\tau = \mu \left(\nabla U + (\nabla U)^T - \frac{2}{3} \delta \nabla \bullet U \right)$$

Total energy eqn. $$\frac{\partial (\rho h_{tot})}{\partial t} - \frac{\partial P}{\partial t} + \nabla \bullet (\rho U h_{tot}) = \nabla \bullet (\lambda \nabla T) + \nabla \bullet (U \bullet \tau) + U \bullet S_M + S_E \quad (4.5)$$

Where h_{tot} is the total enthalpy, related to the static enthalpy *h (T, P)* by:

$$h_{tot} = h + \frac{1}{2} U^2 \quad (4.6)$$

The term $\nabla \bullet (U \bullet \tau)$ represents the work due to viscous stresses and is called the viscous work term. The term $U \bullet S_M$ represents the work due to external momentum sources and is currently neglected.

CFX-Solver is used to launch both solvers and monitor the output. ANSYS Workbench generates the CFX-Solver input file and passes it to ANSYS CFX-Solver Manager. In CFX-Solver first we set the solution units as SI system. Under solution control we set maximum iterations to 10000 and residual type to RMS. Convergence criteria, residual targeted to 1.E-4. In output control, extra output variable set as temperature.

On the Define Run dialog box, Solver Input File is set automatically by ANSYS Workbench. Now we can start the solver run. When the solver run has finished, a completion message appears in a dialog box.

4.5. Obtaining Results in CFX CFD-Post:

CFD-Post is a flexible, state of art post-processor. It is used to allow easy visualization and quantitative analysis of results of CFD simulations. Turbo workspace is used to improve and speed up post-processing for turbomachinery simulation. It includes all the expected plotting objects like, plans, isosurfaces, vectors, streamlines, contours, animations, etc. It allows precise quantitative analysis as, weighted average, forces, results, comparisons, built in and user defined macros. It can create user defined scalar and vector variables. CFD-Post includes automatic reports, charts, and tables.

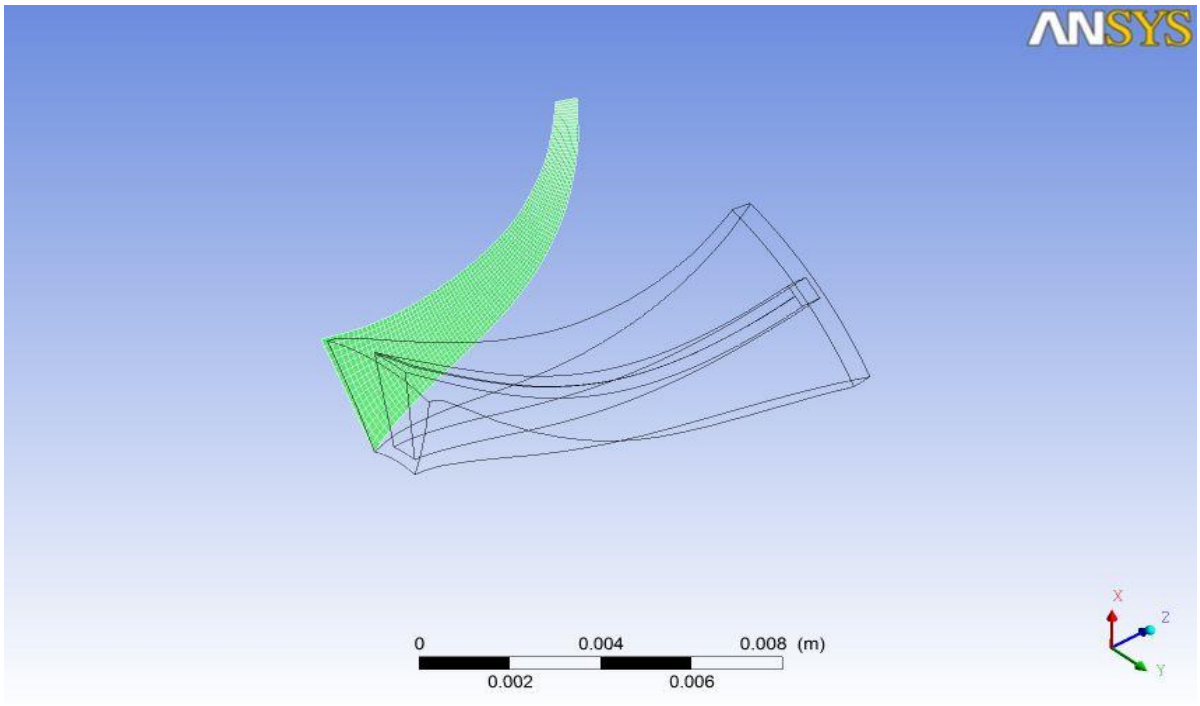

Figure 4.10: Wireframe and Meridional model of turbine rotor

In CFD-Post general workflow, first we prepare locations where data will be extracted from or plots generated. Variables and expression is created to extract data at particular location. Generate qualitative and quantitative data at that location and on the basis of it generate reports to present results.

******

Chapter 5

RESULTS AND DISCUSSION

5. RESULTS AND DISCUSSION:

The computational fluid flow analysis is done in CFD post after completion of cfx simulation. A tabulated result can be seen in generated report. This report gives the variation of different properties from inlet to outlet and hub to shroud, by graphs and counters.

Variations of thermodynamic properties, at different locations of turbine rotor are as following.

Table 5.1: Variations of thermodynamic properties

Quantity	**Inlet**	**LE Cut**	**TE Cut**	**Outlet**	**TE/LE**	**Units**
Density	8.5944	8.4588	4.7636	4.5933	0.5631	[kg m^{-3}]
Pstatic	244299	241899	125866	127695	0.5203	[Pa]
Ptotal	300332	295012	173430	166980	0.5879	[Pa]
Ptotal (rot)	300241	292385	194824	187423	0.6663	[Pa]
Tstatic	95.8298	95.1123	89.6811	88.6704	0.9875	[K]
Ttotal	99.6526	98.5519	96.7926	96.8437	0.9684	[K]
Ttotal (rot)	99.6435	99.6405	99.6466	99.7047	1.0001	[K]
Entropy	5377.19	5385.71	5512.42	5524.16	1.0235	[J kg^{-1} K^{-1}]
Mach (abs)	0.784	0.7449	0.6667	0.6011	0.8949	
Mach (rel)	1.2649	1.1969	0.9175	0.8663	0.7665	
U	186.972	182.671	94.5048	92.5352	0.5173	[m s^{-1}]

From tabulated results we can see that inside the turbine, pressure, temperature, density, velocity and Mach number are decreasing from inlet to outlet while entropy is increasing a little bit from inlet to outlet.

Static temperature of nitrogen available at outlet is 88.67K which is nearly equal to the temperature obtained by S.K. Ghosh [52] during experimental work on turboexpander. Now our output result is validated to experimental results obtained by S.K. Ghosh [52].

Various graphs and contours available from generated results are as following.

5.1 **Pressure variation along streamwise inlet to outlet**:

Static and total pressure variation can be seen from the graph below. Total pressure at inlet and static pressure at outlet is nearly equal to the pressure obtained by S.K. Ghosh [52] experimentally. Total pressure varies from 3bar to 1.6 bar while static pressure varies from 2.4 bar to 1.27 bar along streamline from inlet to outlet of turbine rotor.

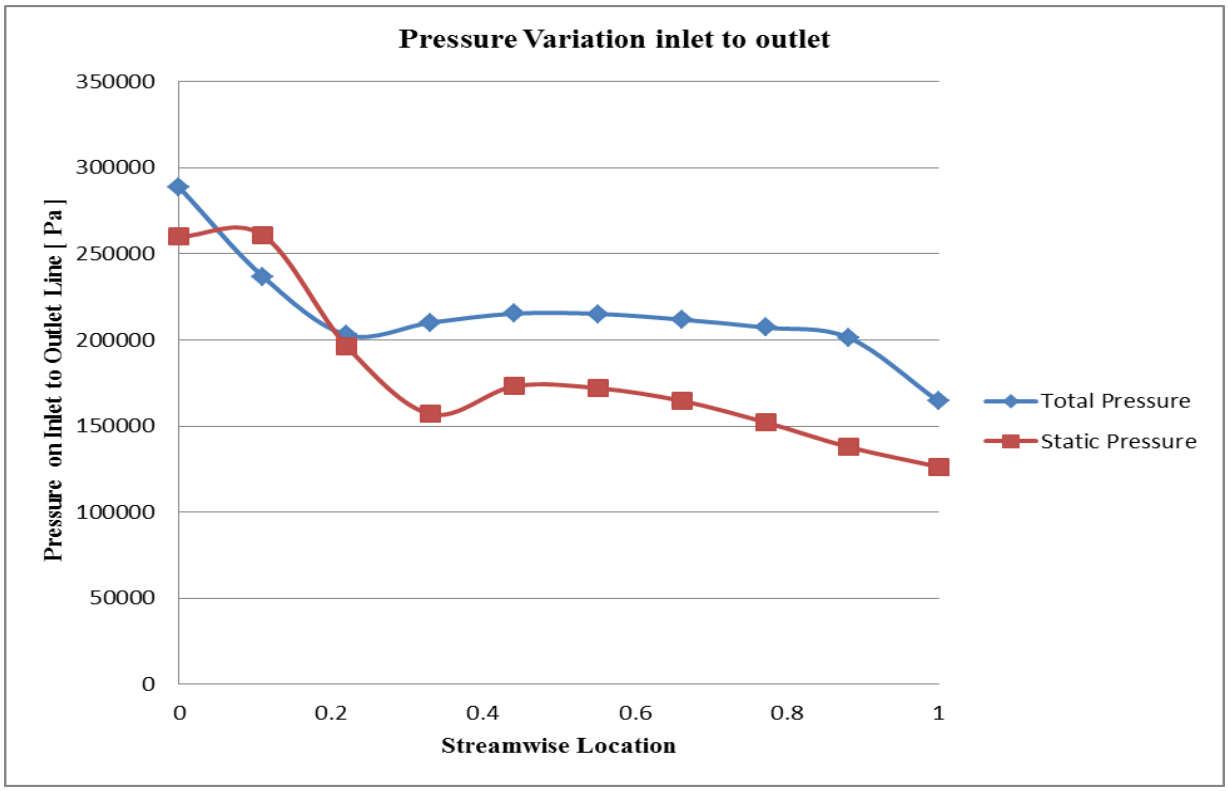

Figure5.1: Pressure variation along streamwise inlet to outlet

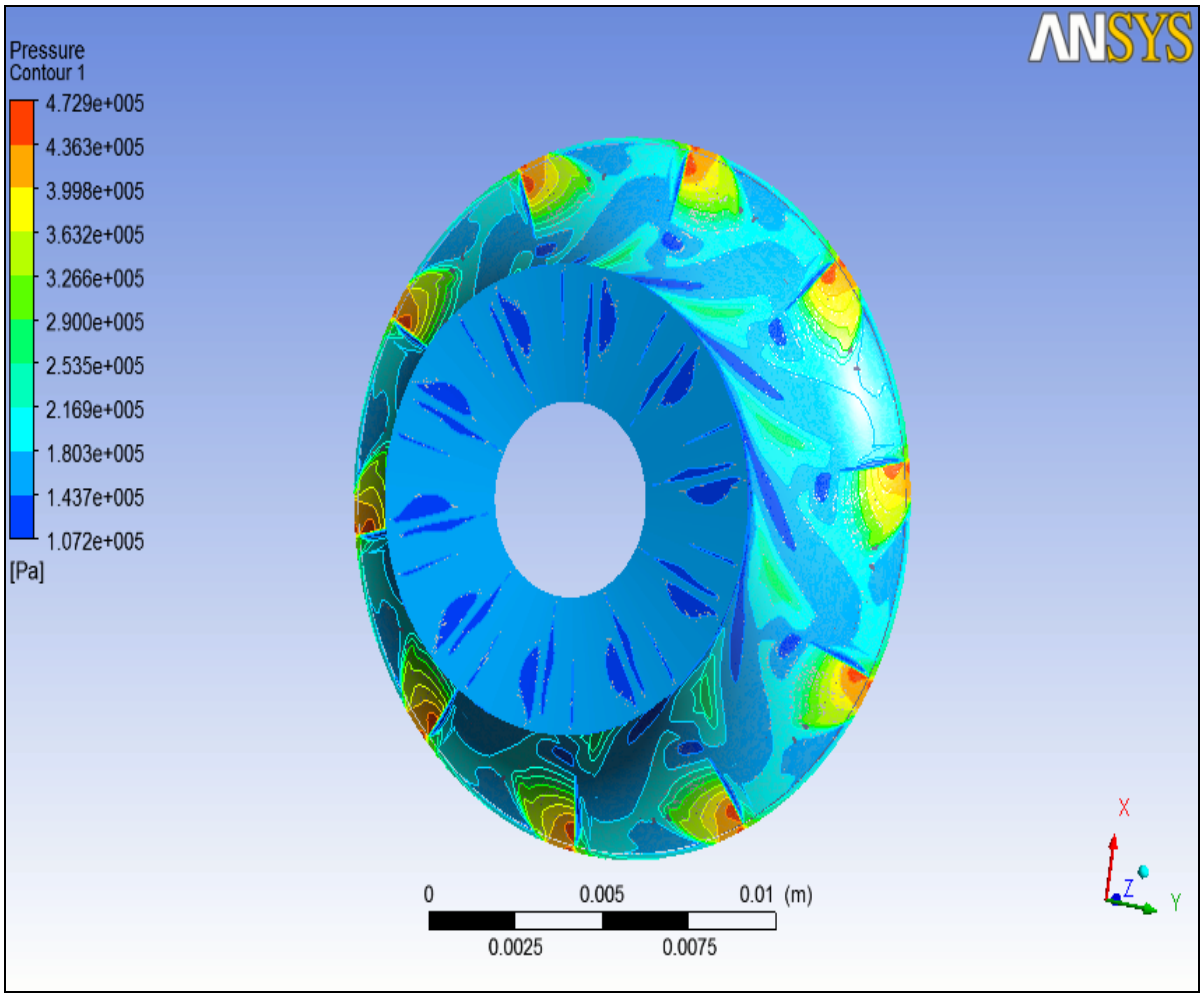

Figure5.2: Isometric 3D view of pressure variation

5.2 Temperature variation along streamwise inlet to outlet:-

Static and total temperature variation can be seen from the graph below. Total temperature at inlet and static temperature at outlet is nearly equal to the temperature obtained by S.K. Ghosh [52] experimentally. Total temperature varies from 99.6K to 96.7K, while static temperature varies from 95.82K to 88.67K along streamline from inlet to outlet of turbine rotor.

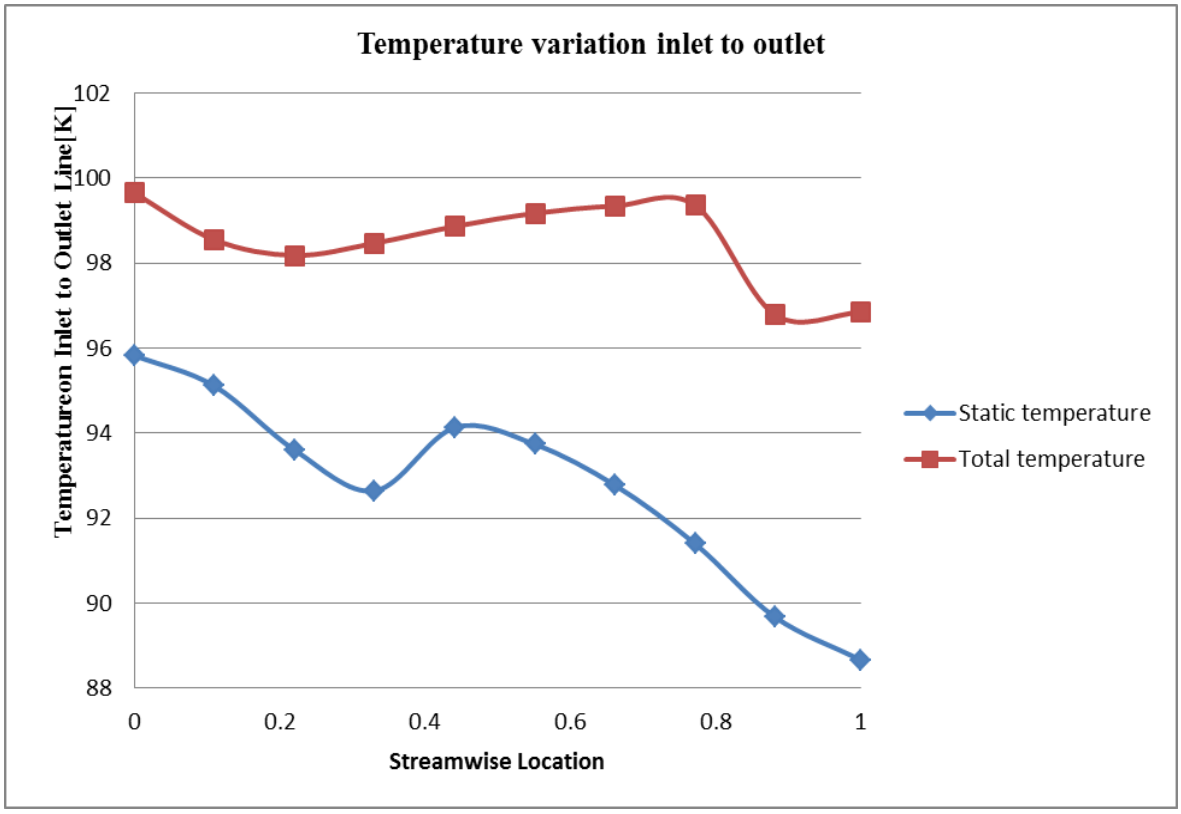

Figure5.3: Temperature variation along streamwise inlet to outlet

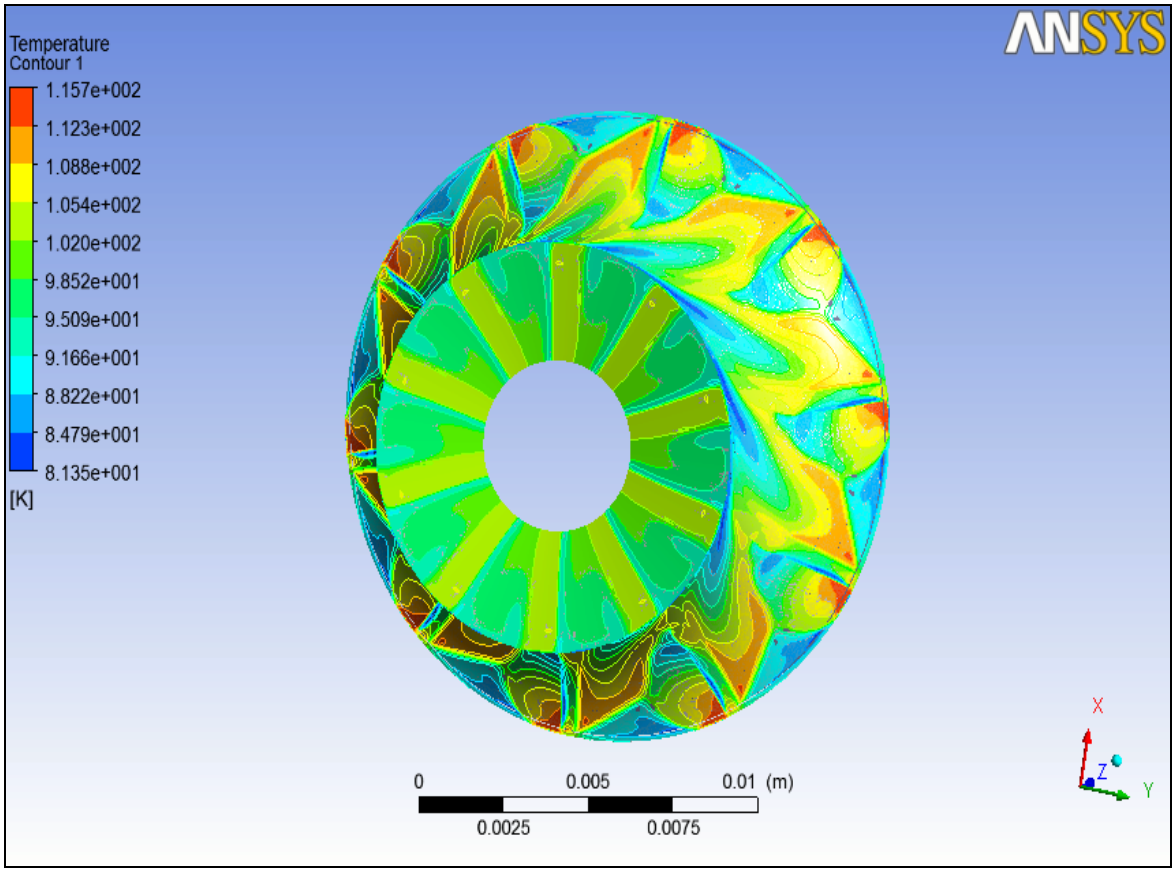

Figure5.4: Isometric 3D view of temperature variation

5.3 Velocity variation along streamwise inlet to outlet:

Velocity variation can be seen from the graph below. Velocity is decreasing inside the turbine from inlet to outlet, 186.90 m/s to 130.146m/s respectively.

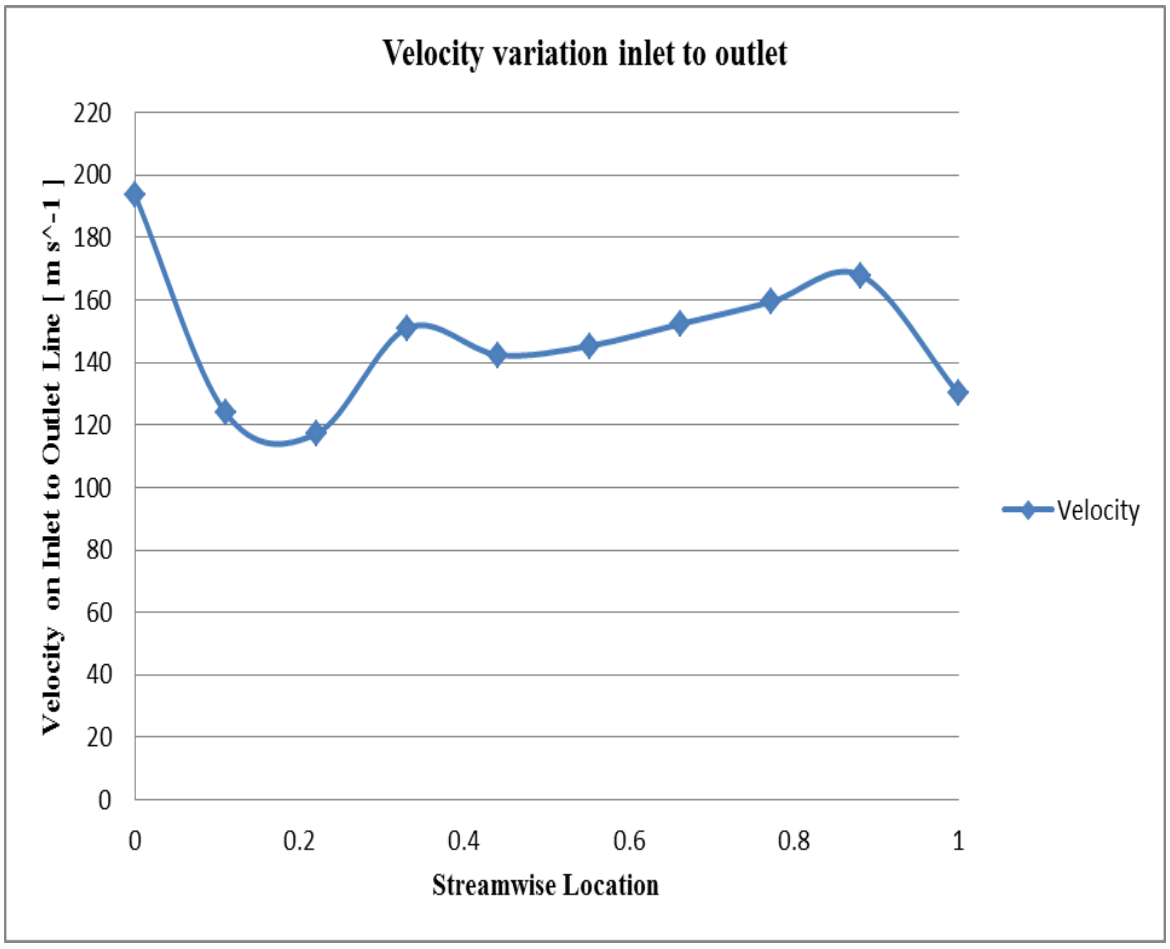

Figure5.5: Velocity variation along streamwise inlet to outlet

5.4 Variation of Mach number along streamwise:

Absolute and relative Mach number variation can be seen from the graph below. Absolute Mach number varies from 0.7 to 0.89, while relative Mach number varies from 1.2 to 0.45 along streamline from inlet to outlet, inside the turbine rotor.

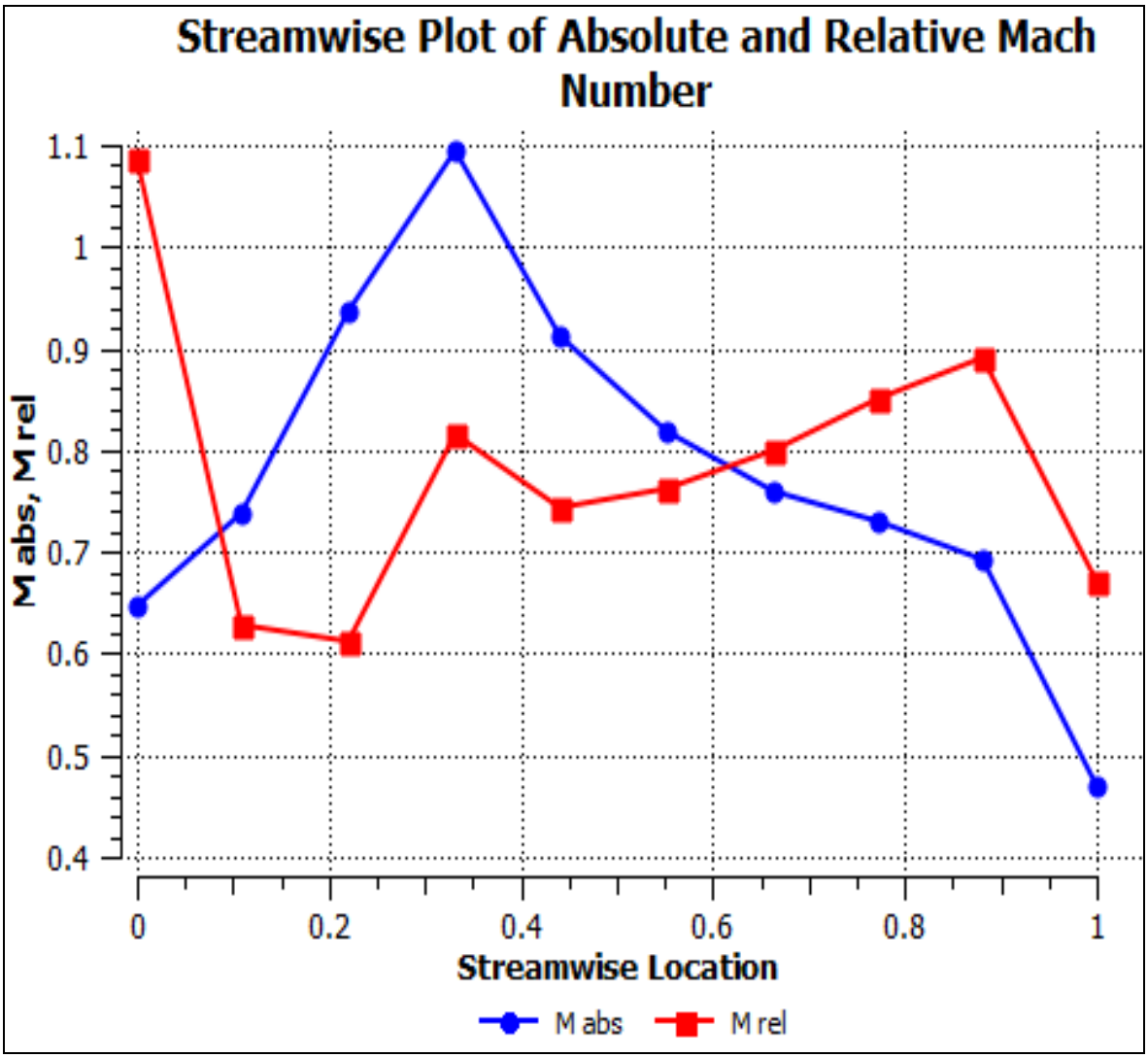

Figure5.6: Variation of Mach number along streamwise

5.5 Variation of density along streamwise inlet to outlet:

Density variation can be seen from the graph below. Density is decreasing inside the turbine from inlet to outlet, 8.59 kg/m^3 to 4.59 kg/m^3 respectively.

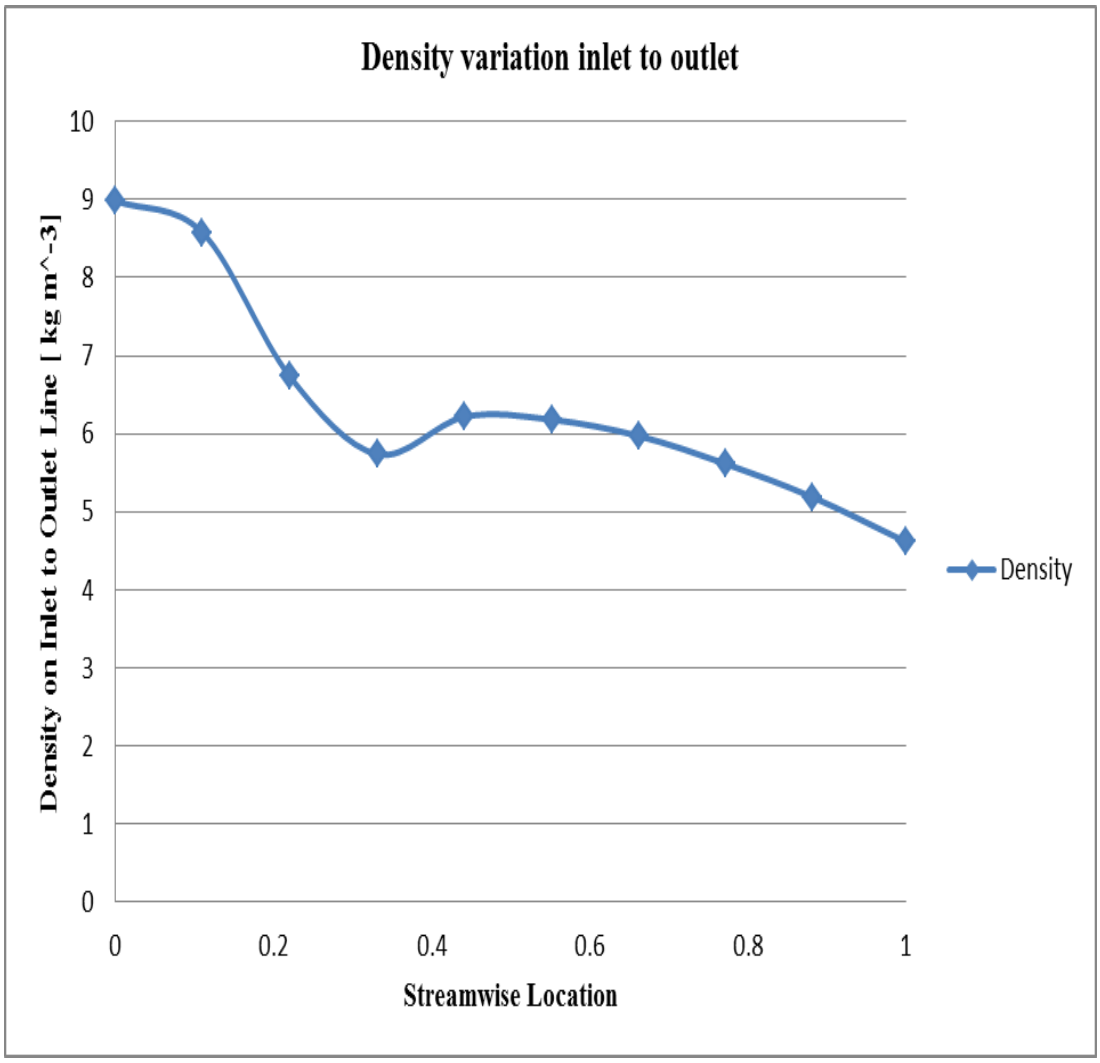

Figure5.7: Variation of density along streamwise inlet to outlet

5.6 Variation of Static Entropy along streamwise:

Static Entropy variation can be seen from the graph below. Static Entropy varies from 5377 J kg^-1 K^-1 to 5524 J kg^-1 K^-1 along streamline from inlet to outlet, inside the turbine rotor, which shows that expansion process is not isentropic. A small increment in entropy can be seen from inlet to outlet, inside the turbine.

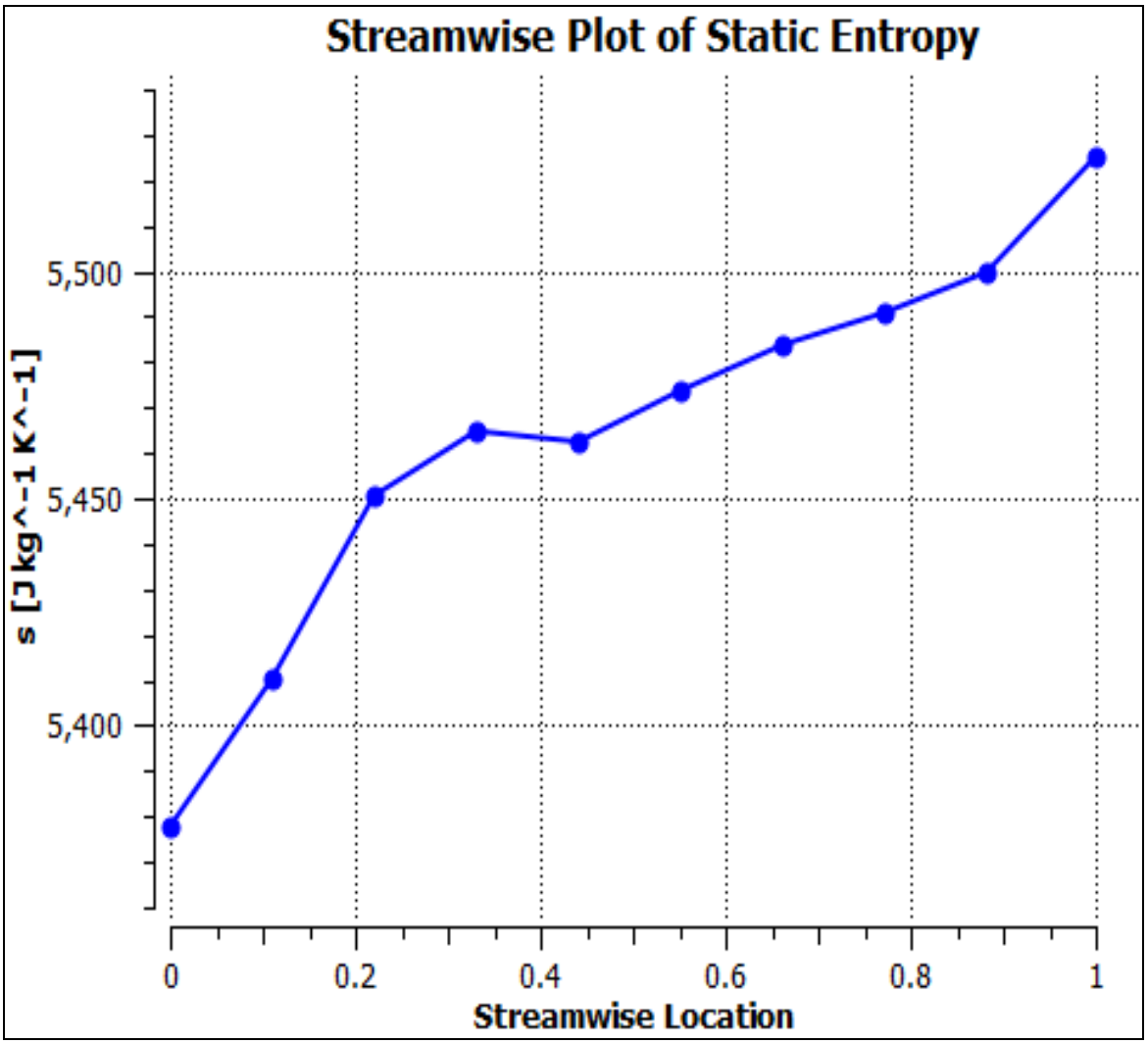

Figure5.8: Variation of Static Entropy along streamwise

5.7 Pressure variation along spanwise hub to shroud:

Pressure variation at different span, hub to shroud can be seen from graph below. At inlet span, hub to shroud variation of pressure is around 2.48 bar to 2.67 bar, while at mid and outlet span pressure is varying around 1.7 bar to 1.8 bar and 1.26 bar to1.27 bar respectively.

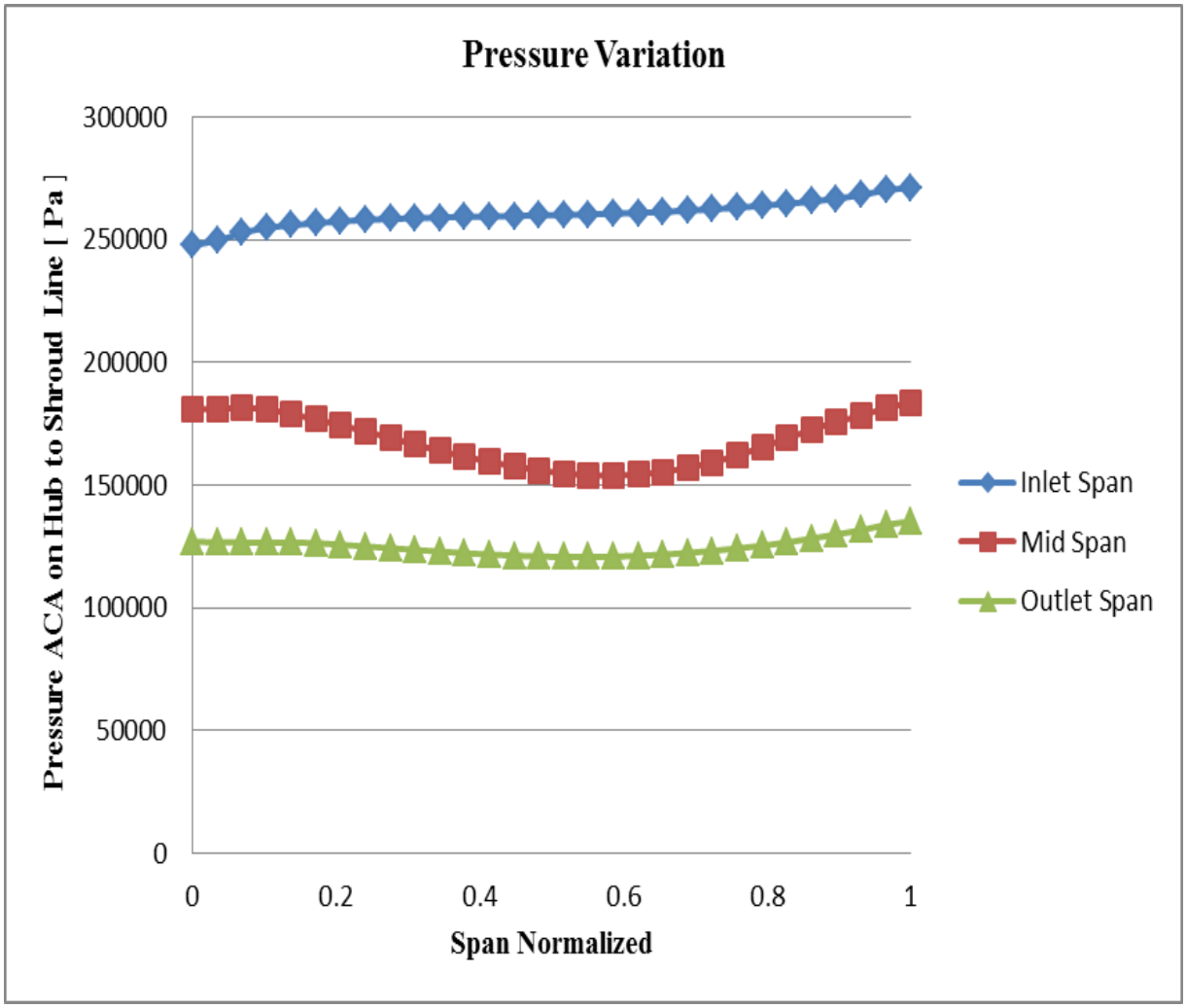

Figure5.9: Pressure variation along spanwise hub to shroud

5.8 Temperature variation along spanwise hub to shroud:

Temperature variation at different span, hub to shroud can be seen from graph below. At inlet span, hub to shroud variation of temperature is around 102 K to 99 K, while at mid and outlet span temperature is varying around 92 K to 94 K and 91 K to86 K respectively.

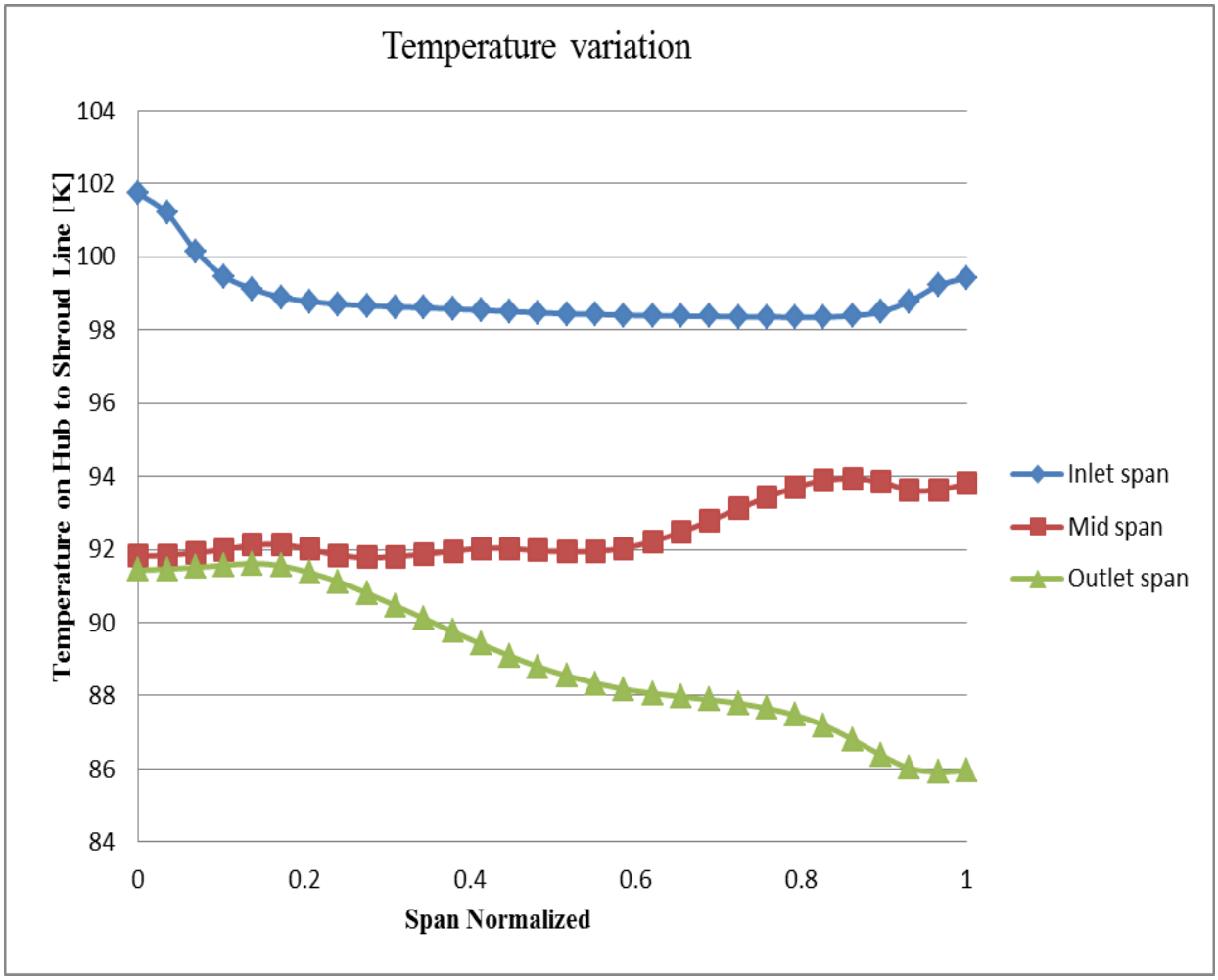

Figure5.10: Temperature variation along spanwise hub to shroud

5.9 Velocity variation along spanwise hub to shroud*:*

Velocity variation at different span, hub to shroud can be seen from graph below. At inlet span, hub to shroud variation of velocity is around 186 m/s to 188 m/s, while at mid and outlet span velocity is varying around 160 m/s to 130 m/s and 90 m/s to100 m/s respectively.

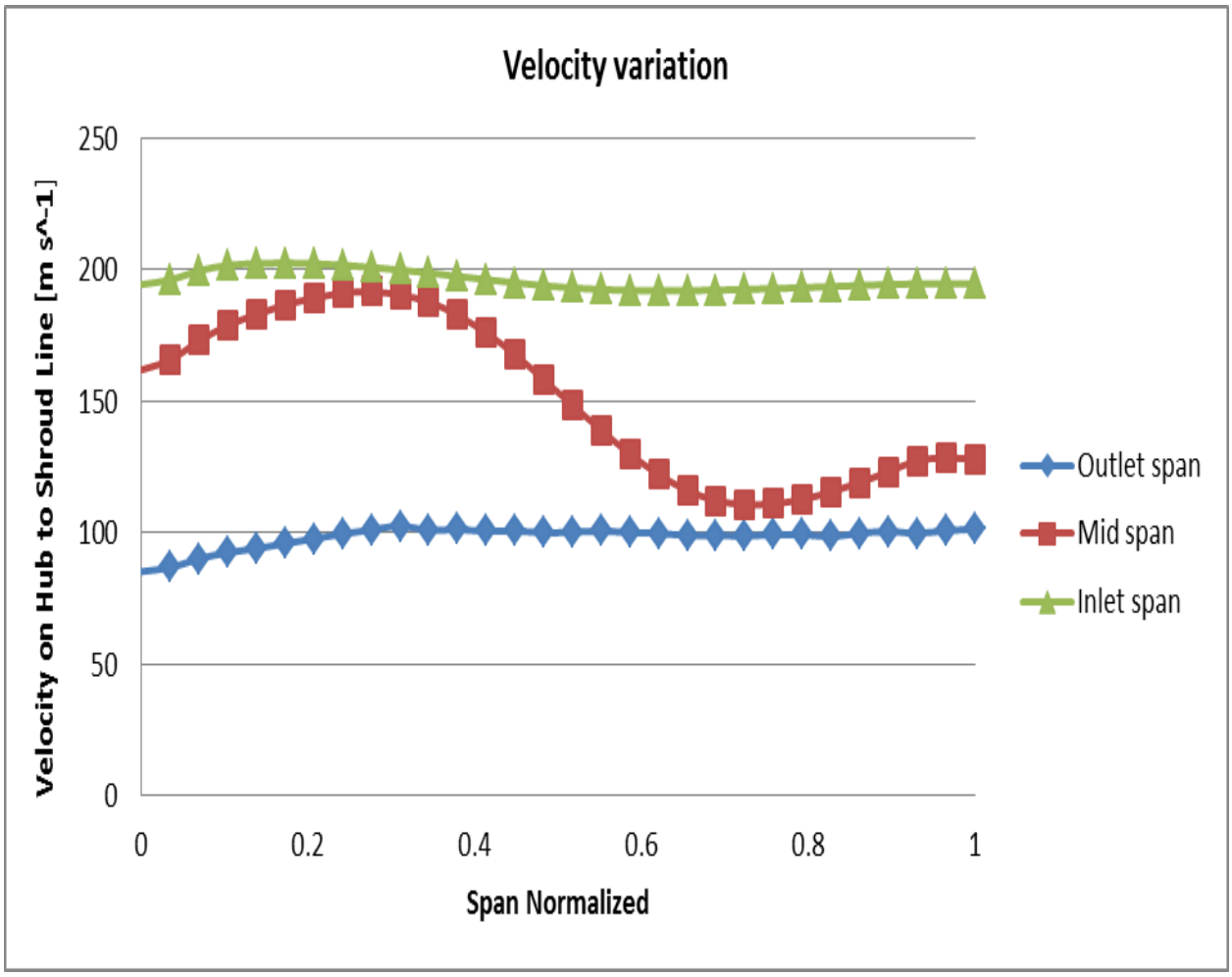

Figure5.11: Velocity variation along spanwise hub to shroud

Observation:-

The gas flows radially inward, is accelerated through inlet guide vanes, and turned. The swirling, high velocity gas enters the expander impeller with relatively low incidence, because the blade tip velocity at the impeller outside diameter approximately matches the gas velocity. Work is extracted from the gas by removing this momentum: as the gas moves inward, it is forced to slow down because the blade rotational velocity decreases with the decreasing radius. The blades also turn the gas to reduce the gas velocity even further. As a result, the gas exits the impeller with low tangential velocity relative to the outside world. In this way, the angular momentum of the gas is efficiently removed. Dew to this reason, different thermodynamic properties decrease from inlet to outlet.

5.10 Blade to blade plots for different spans:

Contour of velocity vector at different Spans:

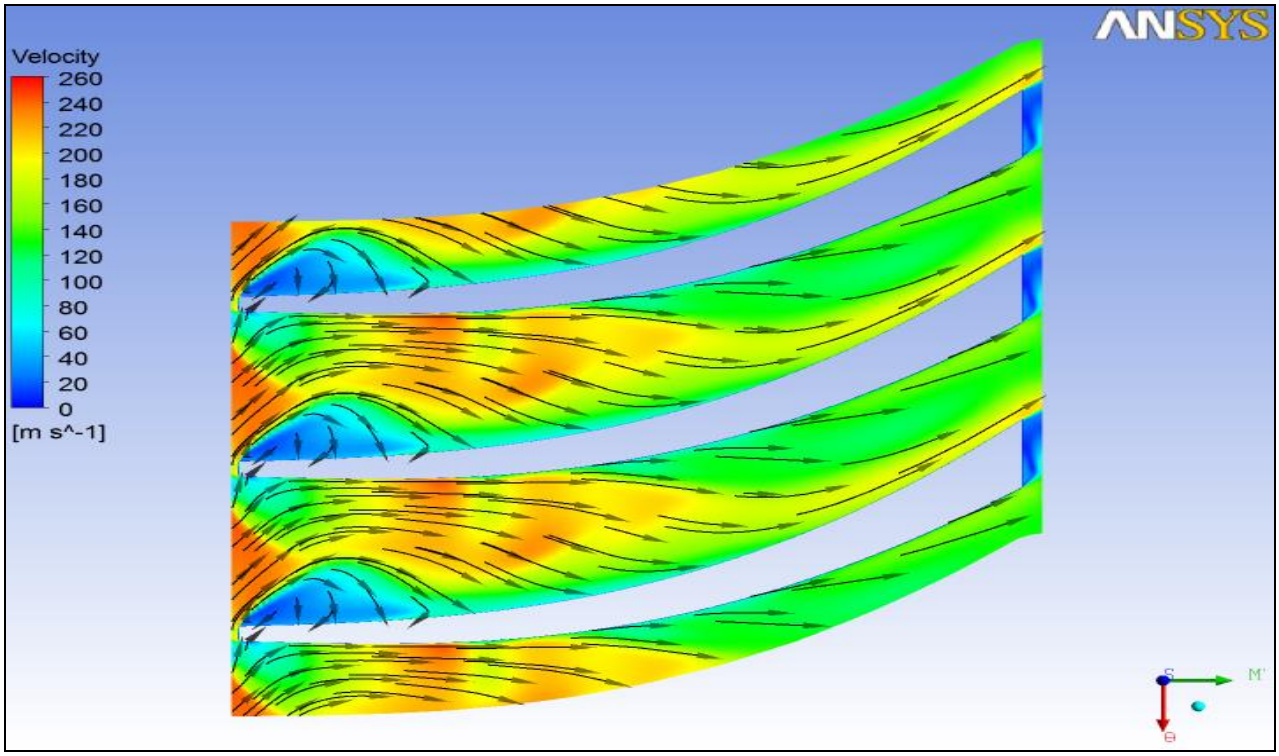

Figure5.12: Velocity Vectors at 20% Span

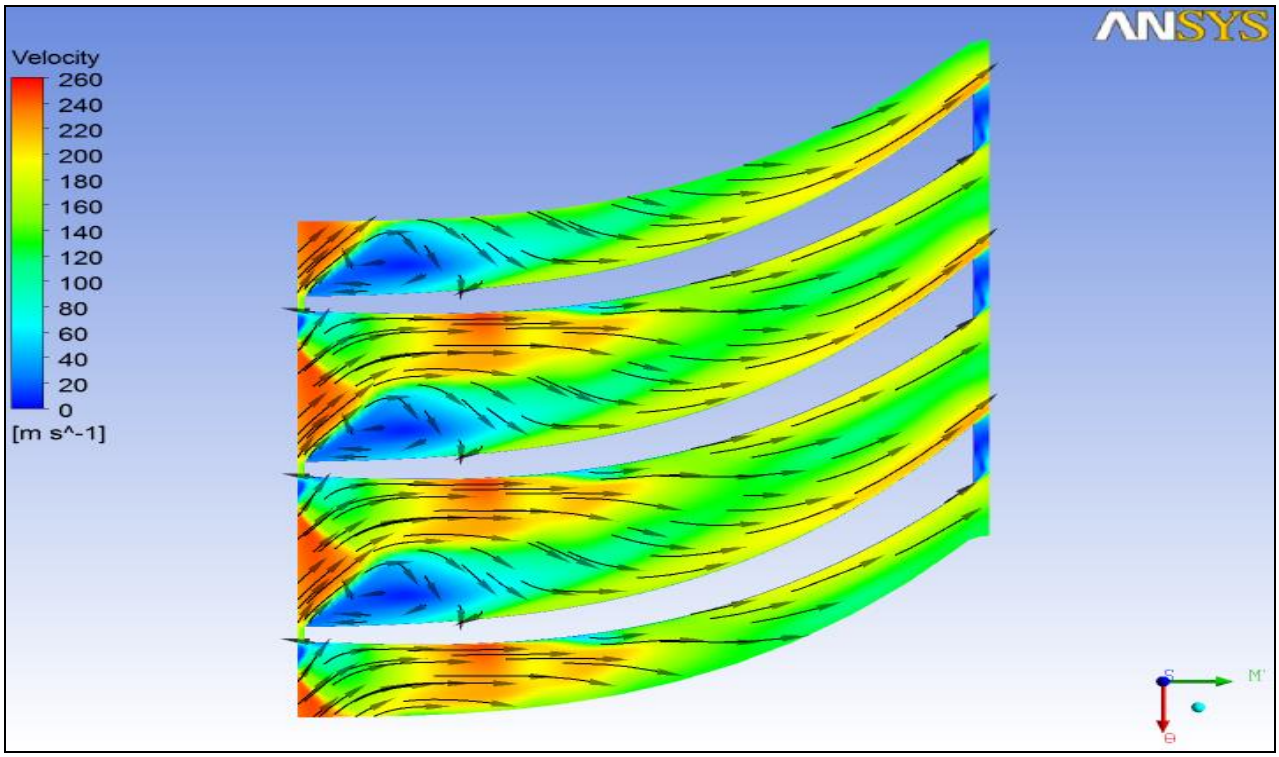

Figure5.13: Velocity Vectors at 50% Span

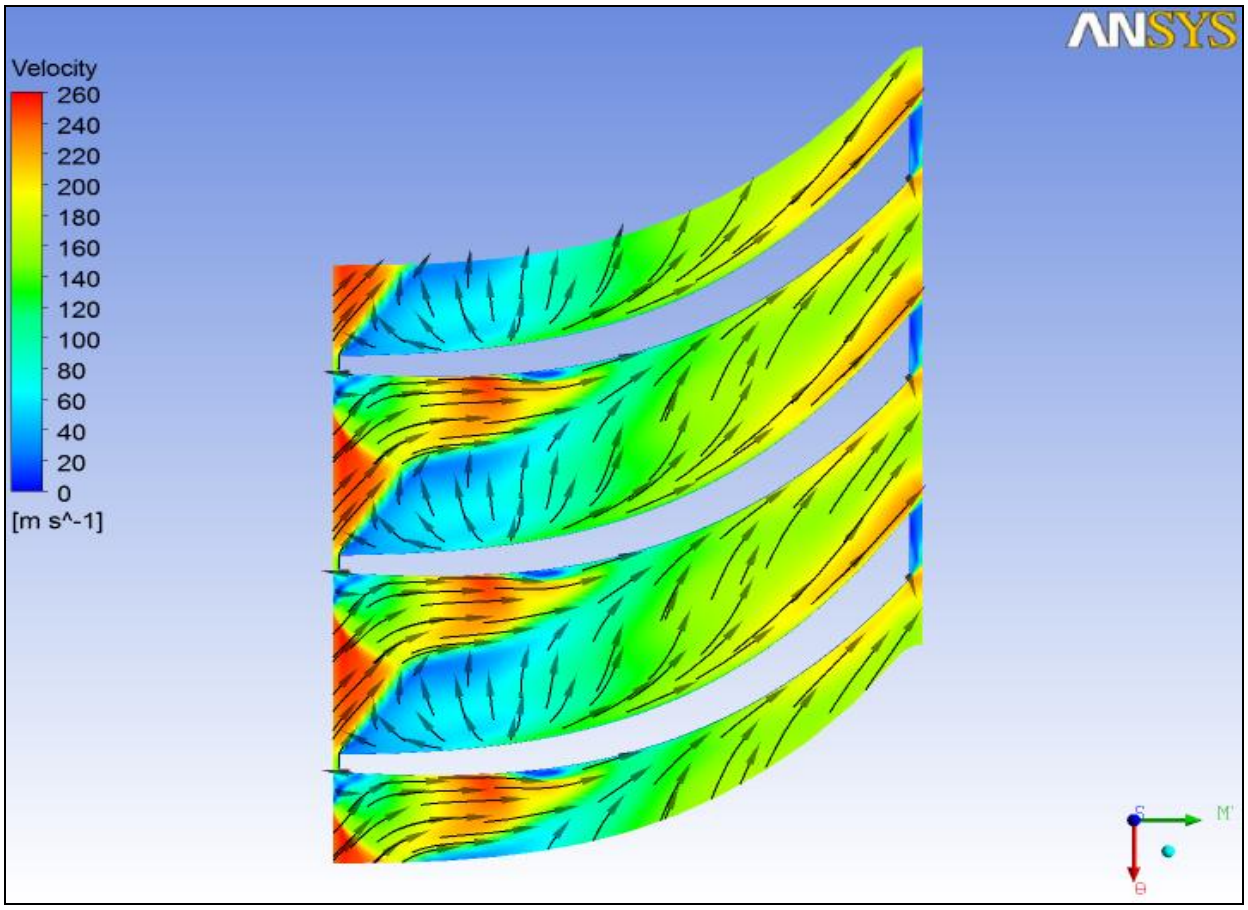

Figure5.14: Velocity Vectors at 80% Span

Observation:-

Above figures are showing the variation of velocity vectors at 20%, 50% and 80% spans from hub to shroud. Here we can see that velocity of fluid is decreasing from inlet to outlet and variation in velocity vectors are more complicate from hub to shroud. At 20% and 50% spans there is less space to move velocity vectors; while at 80% span (near to shroud) variation is more because of gap between blade tip and shroud.

5.11 Meridional Plots:

Contour of Mass Averaged Pressure on Meridional Surface

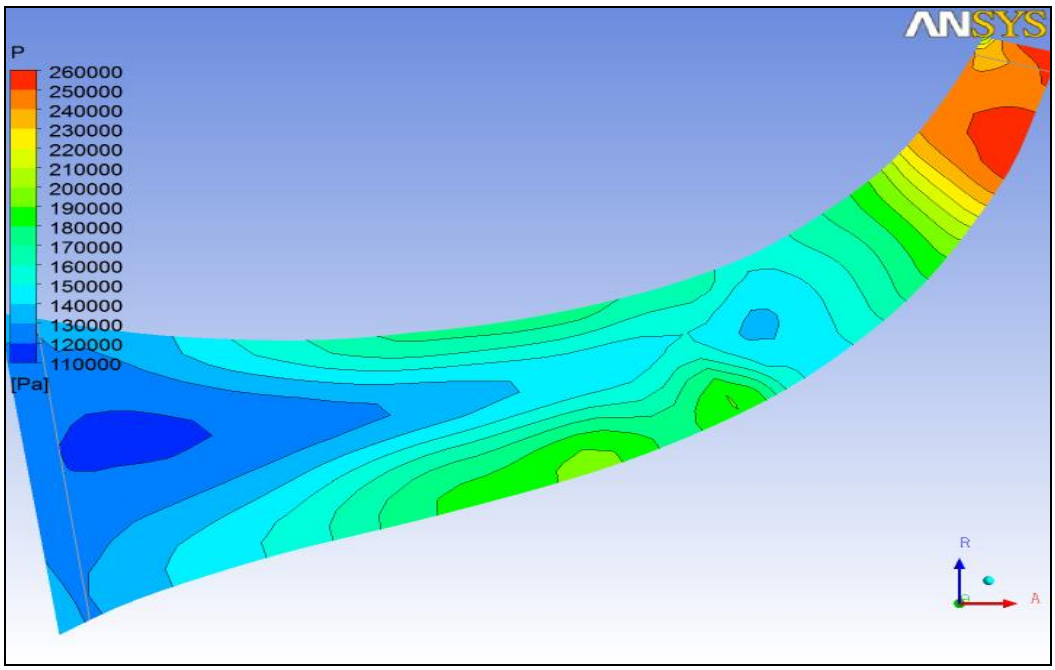

Figure5.15: Mass Averaged Pressure on Meridional Surface

Contour of Mass Averaged Relative Mach number on Meridional Surface:-

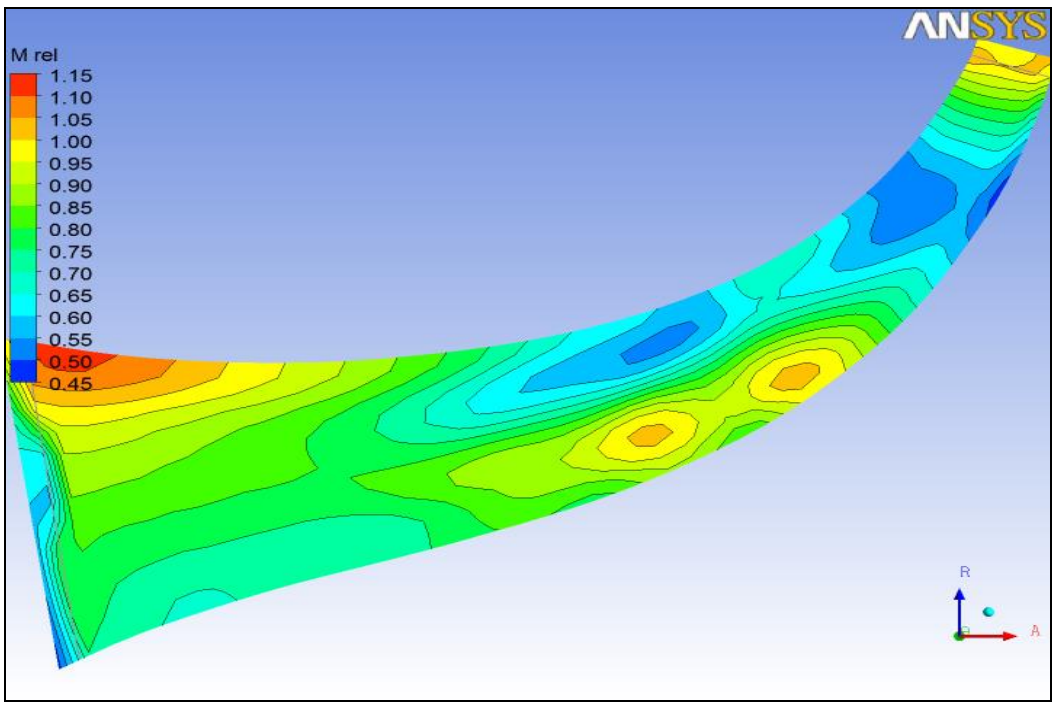

Figure5.16: Mass Averaged Relative Mach number on Meridional Surface

Streamline Plot:-

Velocity Streamlines at Blade Trailing Edge:-

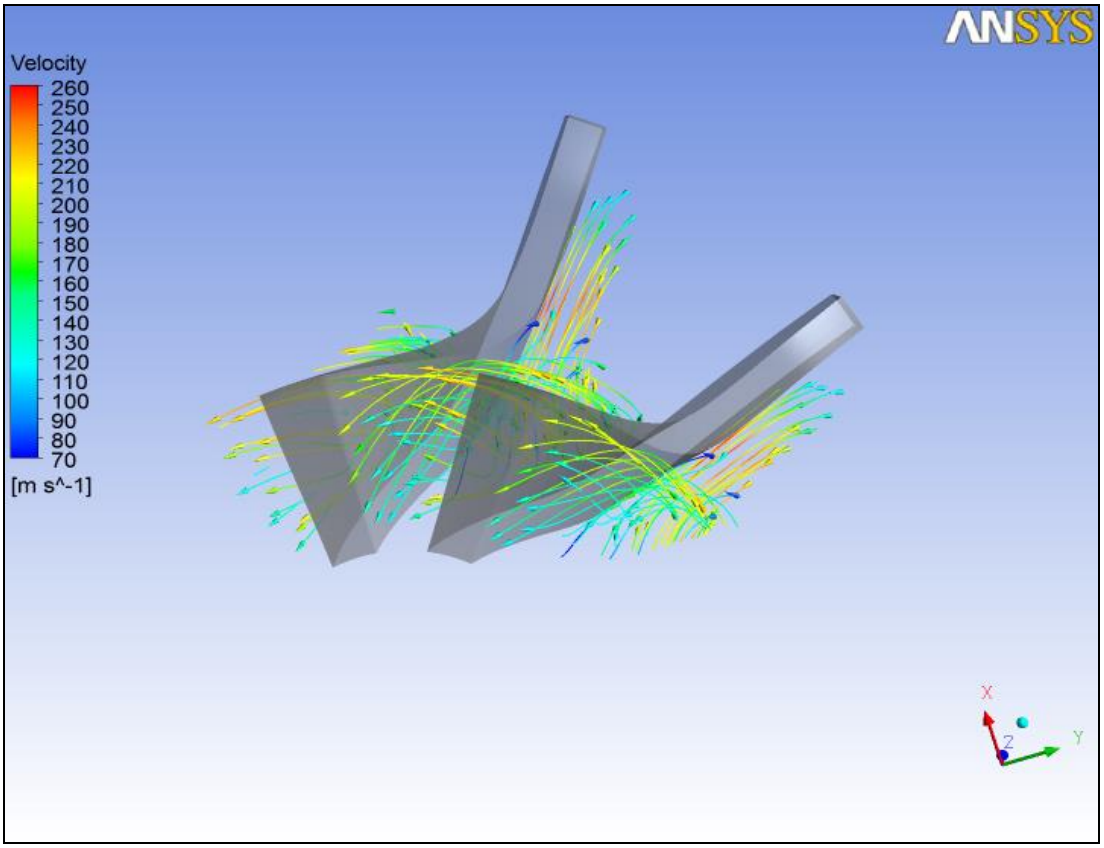

Figure5.17: Velocity Streamlines at Blade Trailing Edge

Observation:-

Meridional plots are showing the variation of pressure and relative Mach number from inlet to outlet. Here we can see that pressure and relative match number are continuously decreasing due to transfer of fluid energy to impeller. As a result, the gas exits the impeller with low pressure and velocity. In fig 5.17 we see that at trailing edge color of streamline is turning to blue, which shows decrease in fluid velocity.

*****

Chapter 6

CONCLUSIONS AND FUTURE WORK

Chapter6

CONCLUSIONS AND FUTURE WORK

6.1. CONCLUSIONS

This work is a modest attempt at flow analyzing inside a cryogenic turboexpander through computational fluid dynamic. A prototype expander has been designed, meshed and simulated using this recipe. The design procedure covers the designing of hub, shroud and blade profile of turboexpander in Bladegen. A cfx model has been developed for flow analysis inside the turbine rotor. The modeling of the various parts of the turbine is done in Bladegen and the computational fluid flow analysis is done using CFX. After validation of output results with experimental results, various graphs and contours indicating the variations of temperature, pressure, velocity, Mach number and entropy inside the turbine along the streamline and spanwise are drawn.

6.2. FUTURE WORK

Future work in this direction will be aimed at computational fluid flow analysis of the remaining parts of turboexpander like nozzle, diffuser, etc. It is expected that a complete model of turboexpander can be computationally analyzed by using proper designing and simulation tools. In this regard, work is planned on the application of CFX tool in mixing plane selection. Once it will be done then computational simulation of different types of turboexpander can be analyzed.

*****

REFERENCES:

[1] **Collins, S.C. and Cannaday, R.L.** Expansion Machines for Low Temperature Processes Oxford University Press (1958).

[2] **Sixsmith, H.** Miniature cryogenic expansion turbines - a review Advances in Cryogenic Engineering (1984), V29, 511-523.

[3] **Swearingen, J. S.** Turbo-expanders Trans AIChE (1947), 43 (2), 85-90

[4] **Clarke, M. E.** A decade of involvement with small gas lubricated turbine & Advances in Cryogenic Engineering (1974), V19, 200-208

[5] **Beasley, S. A. and Halford, P.** Development of a High Purity Nitrogen Plant using Expansion Turbine with Gas Bearing Advances in Cryogenic Engineering (1965), V10B, 27-39

[6] **Swearingen, J. S.** Engineers' guide to turboexpanders RotoFlow Corp, USA, (1970), Gulf Publishing Company

[7] **Voth, R. O., Norton, M. T. and Wilson, W. A.** A cold modulator refrigerator incorporating a high speed turbine expander Advances in Cryogenic Engineering (1966), V11, 127-138

[8] **Colyer, D. B.** Miniature cryogenic refrigerator alternators Advances in Cryogenic Engineering (1968), V13, 405-415

[9] **Colyer, D. B. and Gessner, R. L**. Miniature cryogenic refrigerator Turbomachinary Advances in Cryogenic Engineering (1968), V13, 484-493

[10] **Sixsmith, H.** Miniature expansion turbines, C A Bailey (Ed), Advanced Cryogenics Plenum Press (1971), 225-243

[11] **Schmid, C.** Gas bearing turboexpanders for cryogenic plant 6th International Gas Bearing Symposium University of Southampton England (March 1974) Paper 131 B1: 1-8

[12] **Reuter K. and Keenan B. A.** Cryogenic turboexpanders with magnetic bearings AICHE Symposium Series, Cryogenic Processes and Machinery 89 (294), 35-45

[13] **Izumi, H., Harada, S. and Matsubara, K.** Development of small size Claude cycle helium refrigerator with micro turbo-expander Advances in Cryogenic Engineering (1986), V31, 811 818

[14] **Kun, L. C. and Hanson, T. C.** High efficiency turboexpander in a N2 liquefier AIChE Spring meeting, Houston, Texas (1985)

[15] **Kun, L. C.** Expansion turbines and refrigeration for gas separation and liquefaction Advances in Cryogenic Engineering (1987), V33, 963-973

[16] **Kun, L .C. and Sentz, R. N.** High efficiency expansion turbines in air separation and liquefaction plants International Conference on Production and Purification of Coal Gas & Separation of Air, Beijing, China (1985), 1-21

[17] **Sixsmith, H., Valenjuela, J. and Swift, W. L.** Small Turbo-Brayton cryocoolers Advances in Cryogenic Engineering (1988), V34, 827-836

[18] **Creare Inc, USA** www.creare.com

[19] **Yang, K. J., He, H. B., Ke, G. and Li, G. Y.** Application and test of miniature gas bearing turbines Advances in Cryogenic Engineering (1990), V35, 997-1003

[20] **Sixsmith, H. and Swift, W. A** pair of miniature helium expansion turbines Advances in Cryogenic Engineering (1982), V27, 649-655

[21] **Kato, T., Kamiyauchi, Y., Tada, E., Hiyama, T., Kawano, K., Sugimoto, M., Kawageo, E., Ishida, H., Yoshida, J., Tsuji, H., Sato, S., Xakayama, Y., Kawashima, I.,** Development of a large helium turbo-expander with variable capacity Advances in Cryogenic Engineering (1992), V37B, 827

[22] **Kato, T., Yamaura, H., Kawno, K., Hiyama, T., Tada, E., Kakayama, Y.,Kawashima, I., Sato, M., Yoshida, J., Ito, N., Sato, S. and Shimamato, S. A.** Large scale turboexpander development and its performance test result Advances in Cryogenic Engineering (1990), V35, 1005–1012

[23] **Kato, T., Miyake, A., Kawno, K., Hamada, K., Hiyama, T., Iwamoto, S., Ebisu, H., Tsuji, H., Saji, N., Kaneko, Y., Asakura, H., Kuboto, M. and Nagai, S.** Design and 160 test of wet type turbo-expander with an alternator as a brake Advances in Cryogenic Engineering (1994), V39, 917-92

[24] **Ino, N., Machida, A. and Ttsugawa, K.** Development of high expansion ratio He turboexpander Advances in Cryogenic Engineering (1992), V37B, 835-844

[25] **Ino, N., Machida, A. and Ttsugawa, K.** Development of externally pressurized thrust bearing for high expansion ratio expander Advances in Cryogenic Engineering (1992), V37B, 817-825

[26] **Baranov, A., Duzev, V., Kashirskikh, G., Mikhailov, A., Ugrovatov, A. and Zhulkin, V.** An experience in the maintenance of a liquefier from the T-15 cryogenic system, results of its reliability and capacity enhancement Advances in Cryogenic Engineering (1996), V41A, 737-743

[27] **Cryogenic Industries** FrostByte - newsletter (Dec 1995)

[28] **ACD Inc., USA**, www.acdcom.com

[29] **Aghai, R. R., Lin, M.C. and Ershaghi, B.** High Performance cryogenic turboexpanders Advances in Cryogenic Engineering (1996), V41, 941-947

[30] **Aghai, R. R., Lin, M.C. and Ershaghi, B.** Improvements of the efficiency of the turboexpanders in cryogenic applications Advances in Cryogenic Engineering (1996), V41, 933-940

[31] **Fuerest, J. D.** Experience with small turbomachinery in a 400 W refrigerator Advances in Cryogenic Engineering (1996), V41, 949-955

[32] **Sixsmith, H., Hasenbin, R. and Valenjuela, J. A.** A miniature wet turboexpander Advances in Cryogenic Engineering (1990), V35, 989-995

[33] **Xiong Lian-You Hou, Y., Wang, J., Lin, M. F., Wu, G., Wang, B. C. and Chen, C. Z.** A easibility study on the use of new gas foil bearings in cryogenic turboexpander Advances in Cryogenic Engineering (1998), V43, 662-666

[34] **L'Air Liquide, France** www.airliquide.com

[35] **Marot, G. and Villard, J. C.** Recent developments of air liquide cryogenic expanders Advances in Cryogenic Engineering (2000), V45, 1493-1500

[36] **Jadeja, H. T., Mitter, A. and Chakrabarty, H. D.** Turboexpander application for cryoprocessing of nitrogen and related gases Proceedings of INCONCRYO85 Indian Cryogenic Council Tata McGraw (1985), 85-101

[37] **Mitter, A., Jadeja, H. T. and Chakrabarty, H. D.** Mechanical reliability and manufacturing process for indigenous development of turboexpander Proceedings of INCONCRYO-88 Indian Cryogenic Council (1988), 331-337 161

[38] **Ghosh, P.** Analytical and Experimental Studies on Cryogenic Turboexpanders Ph.D dissertation, IIT Kharagpur

[39] Akhtar M. S. Selection and Optimisation of Centrifugal Compressors for oil and gas applications. Using computers in the design and selection of fluid machinery I.Mech.E (1993), 29-41

[40] **von der Nuell , W. T.** Single - stage radial turbine for gaseous substances with high rotative and low specific speed Trans ASME (1952), V74, 499-515

[41] **Balje, O. E.** A contribution to the problem of designing radial turbomachines Trans ASME (1952), V74, 451-472

[42] **Balje, O. E.** A study on design criteria and matching of turbomachines: Part-A—similarity relations and design criteria of turbines Trans ASME J Eng Power (1972), 83-101

[43] **Cartwright, W. G.** Specific speed as a measure of design point efficiency and optimum geometry for a class of compressible flow turbomachines Scaling for performance prediction in rotordynamic machines I Mech E (1978), 139-145

[44] **Balje, O. E.** A study on design criteria and matching of turbomachines: part-b--compressor and pump performance and matching of turbocomponents Trans ASME J Eng Power (1972), 103-114

[45] **RohliK, Harold E.** Analytical determination of radial inflow turbine geometry for maximum efficiency NASA TN D-4384 (1968)

[46] **Luybli, R. E. and Filippi, R. E.** Performance options for cryogenic turboexpander AIChE symposium on Creyogenic properties, processes and applications (1986) V82, 24-33

[47] **Vavra, M. H.** The applicability of similarity parameters to the compressible flow in radial turbomachines Proc Ins Mech Eng Internal Thermodynamics (Turbomachine 1970), 118- 132

[48] **Whitfield, A.** Non-dimensional conceptual design of radial inflow turbines Radial Turbines Part B: Application of empirical correlations

[49] **Denton, J. D.** The turboexpander - a design, make and test student project ASME-96-GT-191 (1996)

[50] **Wallace, F. J.** Theoretical assessment of the performance characteristics of inward radial flow turbines Trans ASME (1958), 931-952

[51] **Hasselgruber, H.** Stromungsgerechte gestaltung der laufrader von radialkompressoren mit axialem laufradeintrict Konstruction (1958), 10(1) 22(in German)

[52] **Ghosh, S.k. "**Experimental and Computational Studies on Cryogenic Turboexpander*"* Ph.D dissertation, NIT Rourkela.

[53] **Ghosh, S.K., Sahoo, R.K., Sarangi, S.K.** "Computational Geometry for the Blades and Internal Flow Channels of Cryogenic Turbine."

[54] **Ghosh, S.K., Seshaiah, N., Sahoo, R.K., Sarangi, S.K.** Design of Turboexpander for Cryogenic applications**,** Indian Journal of Cryogenics, Special Issue - Vol.2, 75-81, (2005).

*****